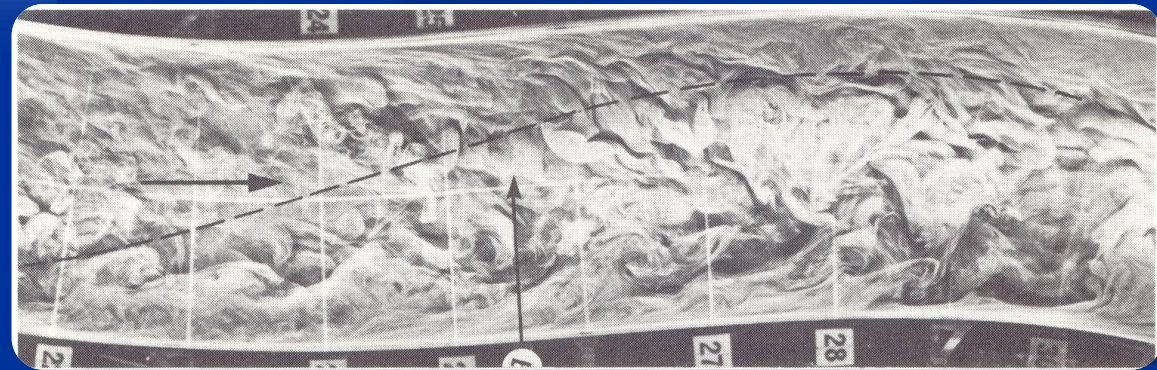


# LARGE-SCALE RIVER TURBULENCE AND ITS MORPHOLOGICAL CONSEQUENCES

A.M. Ferreira da Silva

Queen's University  
Kingston, Ontario  
Canada



# Alternate Bars (or one-row bars): Definition and Geometric Properties



Experiments by  
Kinoshita 1961



Experiments  
at Queen's



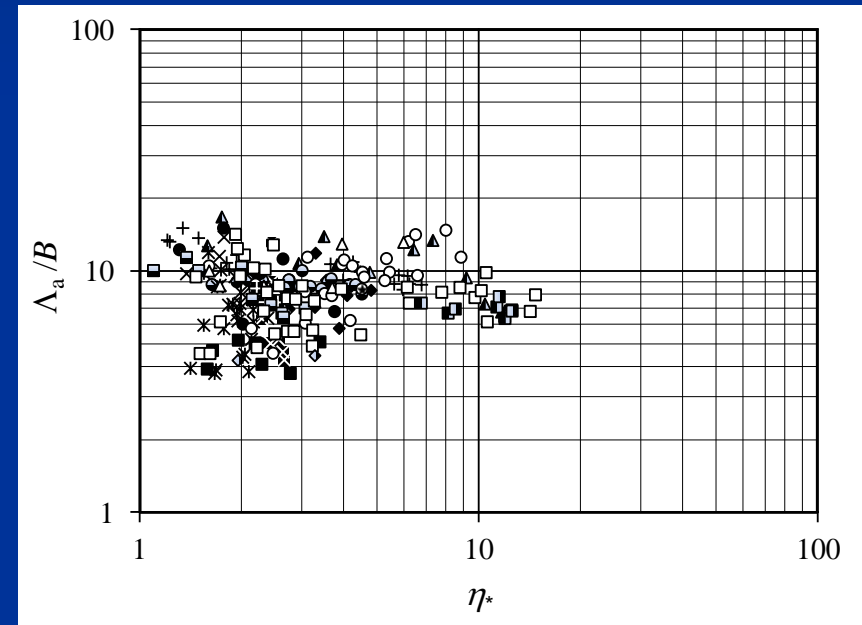
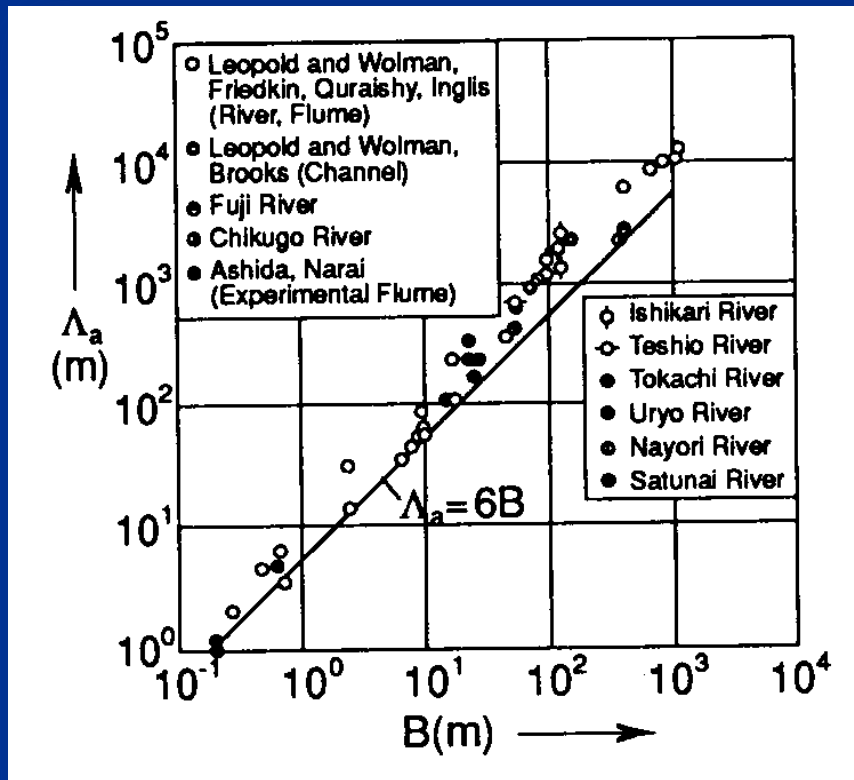
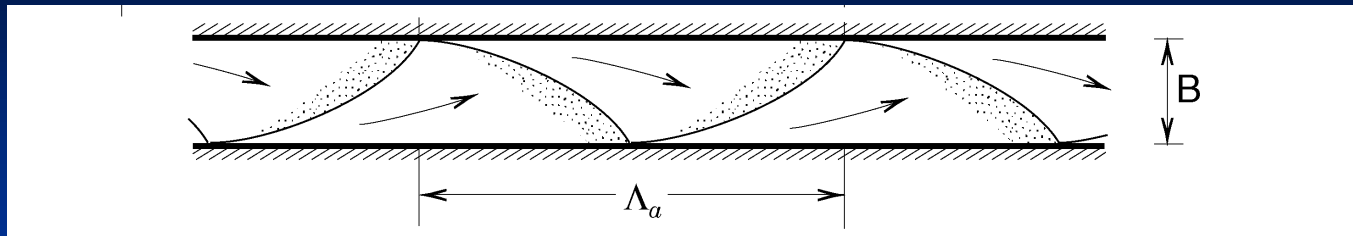
Naka River, Japan



Rio Coto, Costa Rica

- Large-scale, migrating bed forms, characterized by diagonal crests, implying a pattern of alternating holes along the sidewalls

# Alternate Bars: Definition and Geometric Properties



From Boraey (2014)

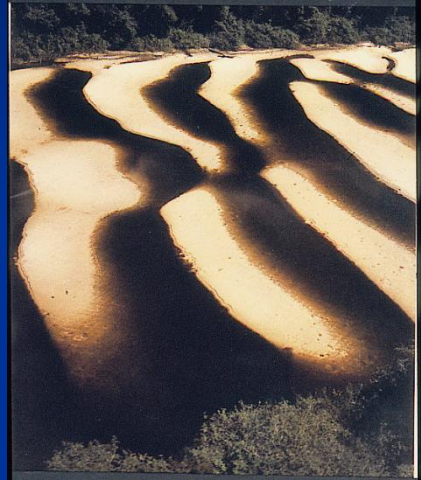
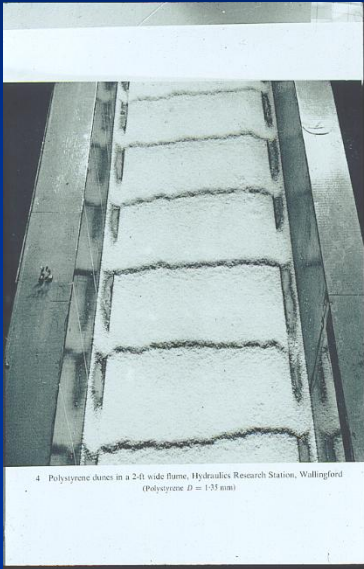
From Yalin (1992);  
River Mechanics

Yalin (1992)  $\longrightarrow$

$$\Lambda_a \approx 6B$$

# Alternate Bars: Definition and Geometric Properties

Dunes



$$\Lambda_d \approx 6h$$

Kishi (1980) and Jaeggi (1984):

Alternate bars are a horizontal counterpart of dunes



# Alternate Bars: Relationship to Meandering

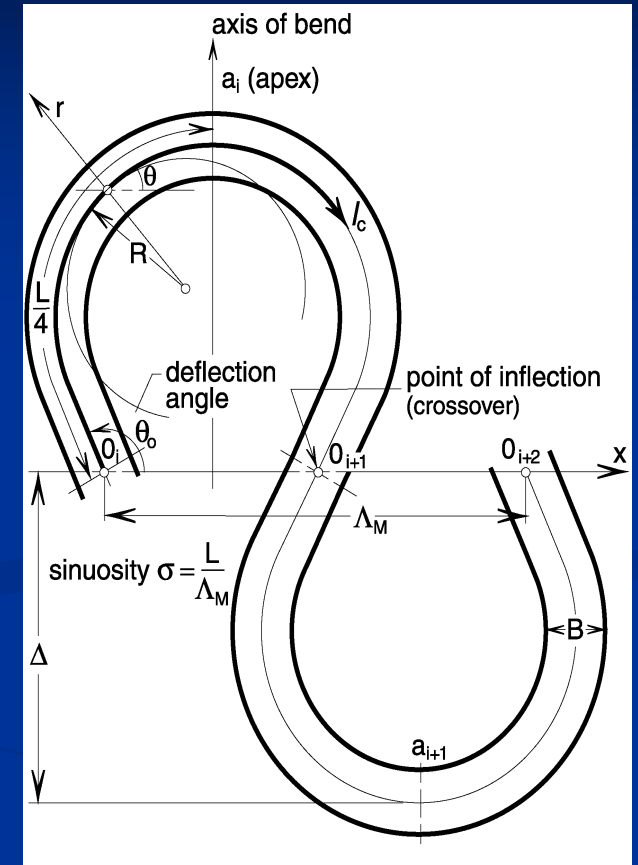
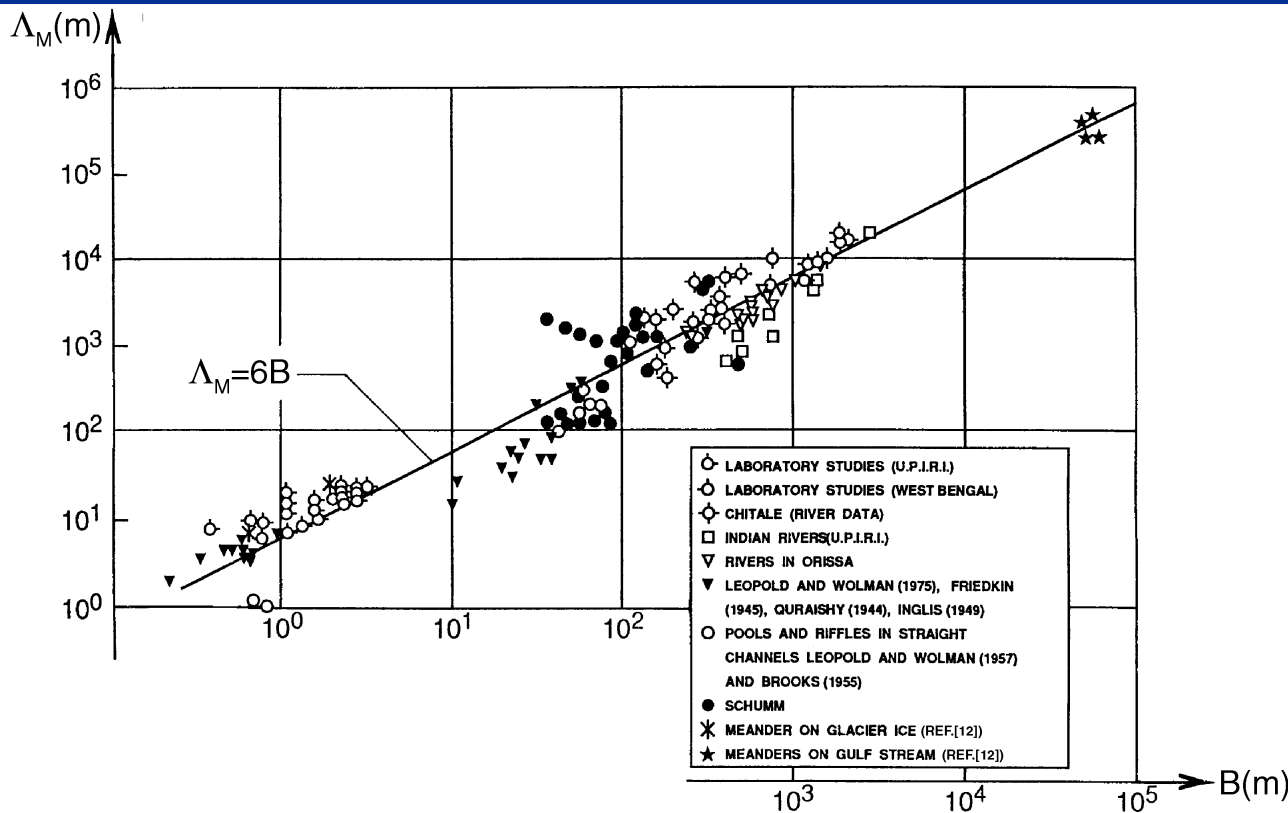


Columbia River



Tributary of the Nelson River, Hudson Bay, Canada

# Alternate Bars: Relationship to Meandering

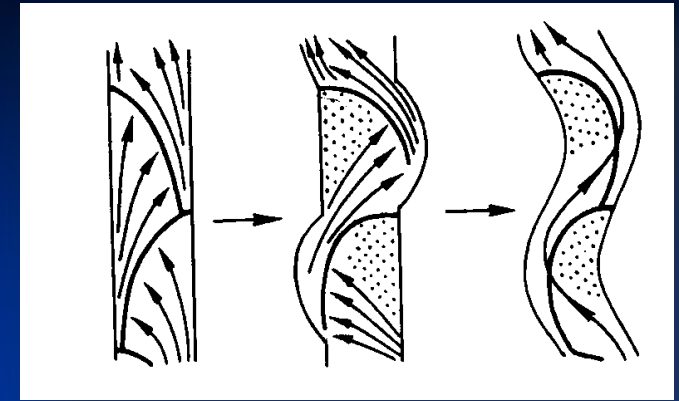


From Yalin and da Silva (2001), Fluvial Processes Monograph; after Garde and Raju (1977)

$$\Lambda_a \approx \Lambda_M \approx 6B$$

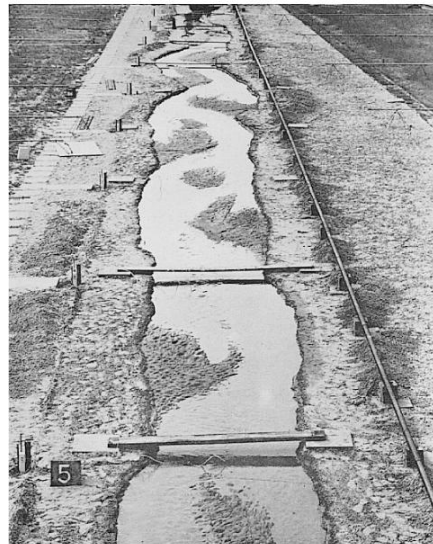
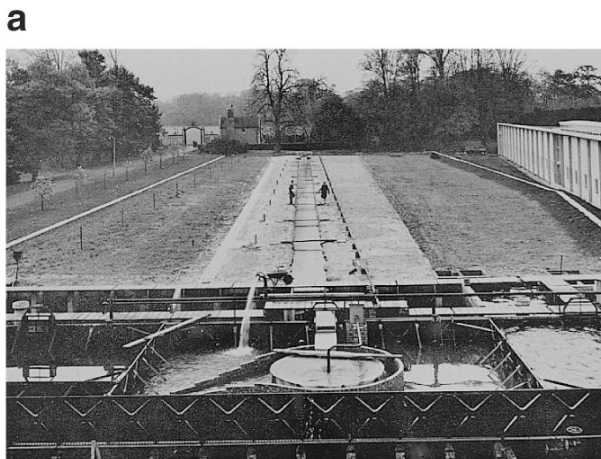
# Alternate Bars: Origin

Prevailing view throughout the 1970's and 80's:  
alternate bars were the cause for meandering

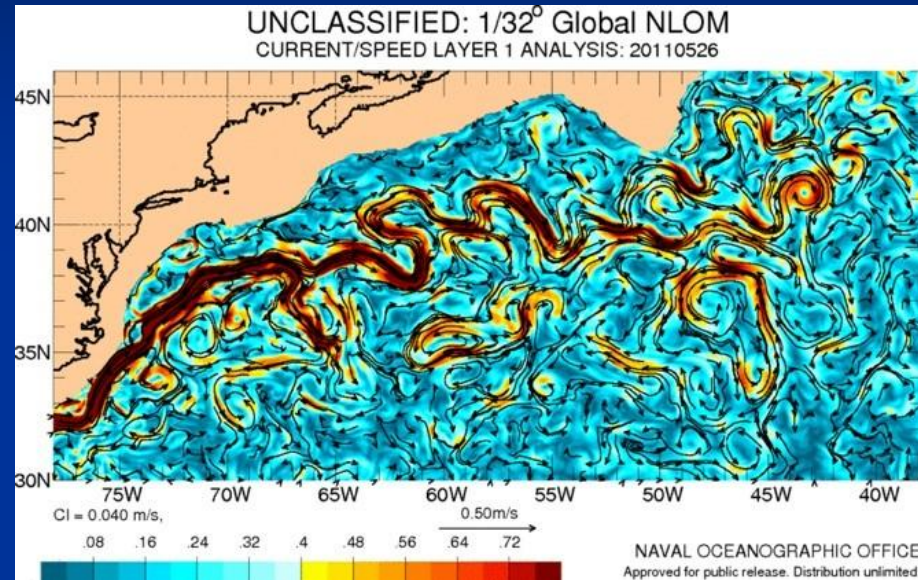
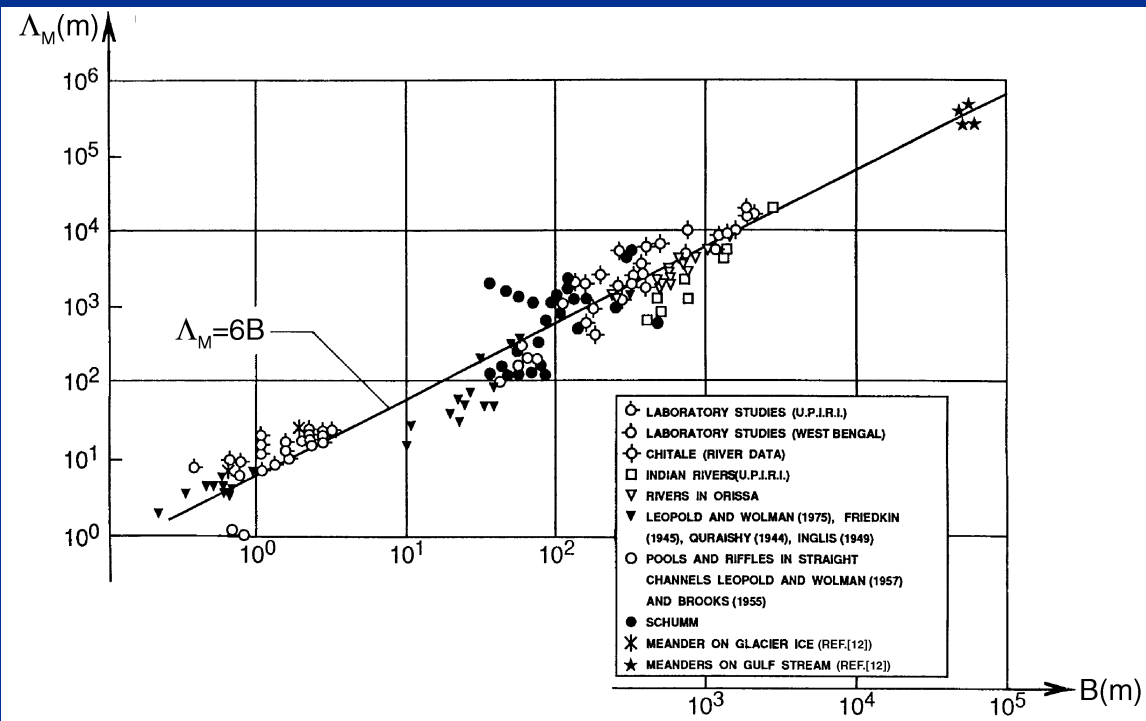


From Sukegawa (1970)

HR Wallingford, 1960's, P. Ackers, J.A. Charlton  
(experiments on the formation of meandering) ↓



# Alternate Bars: Origin



Meanders in the Gulf Stream

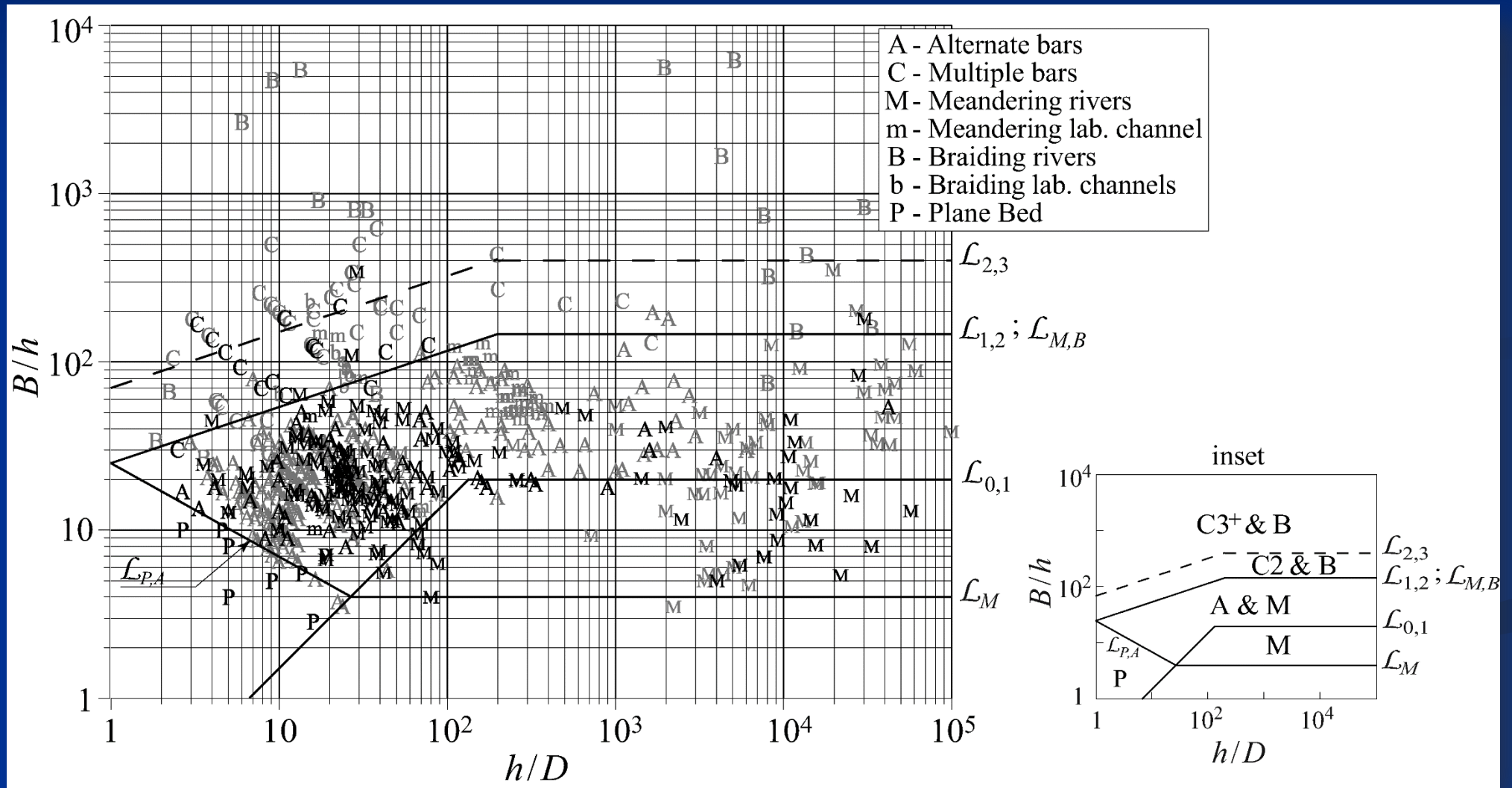
From Yalin and da Silva (2001), Fluvial Processes Monograph; after Garde and Raju (1977)

$$\Lambda_a \approx \Lambda_M \approx 6B$$




# Alternate Bars: Origin

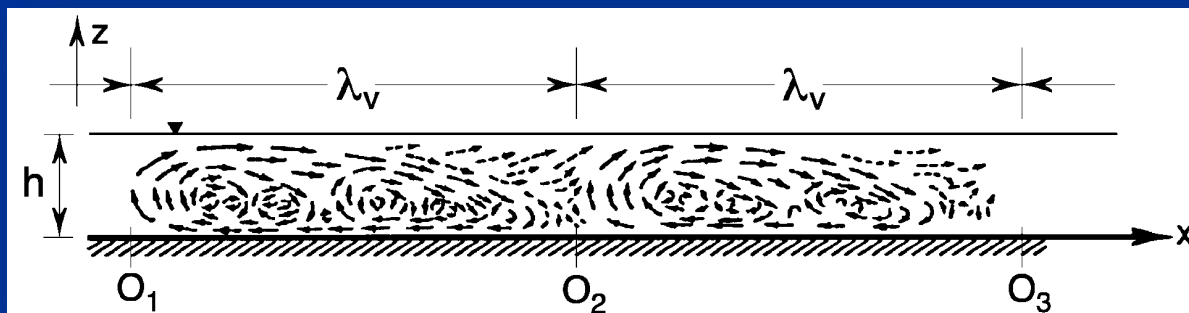
( $B/h; h/D$ ) – plan of Yalin and da Silva 2001; Existence region plan of alternate bars



# Turbulence Coherent Structures

Near wall phenomenon  large-scale CS's (in a variety of flows) extending throughout the body of fluid (Grass 1971, Hussain 1983, Talmon et al. 1986, Rashidi and Banerjee 1988, Nezu and Nakagawa 1993, Jimenez 1998, Roy et al. 1994)

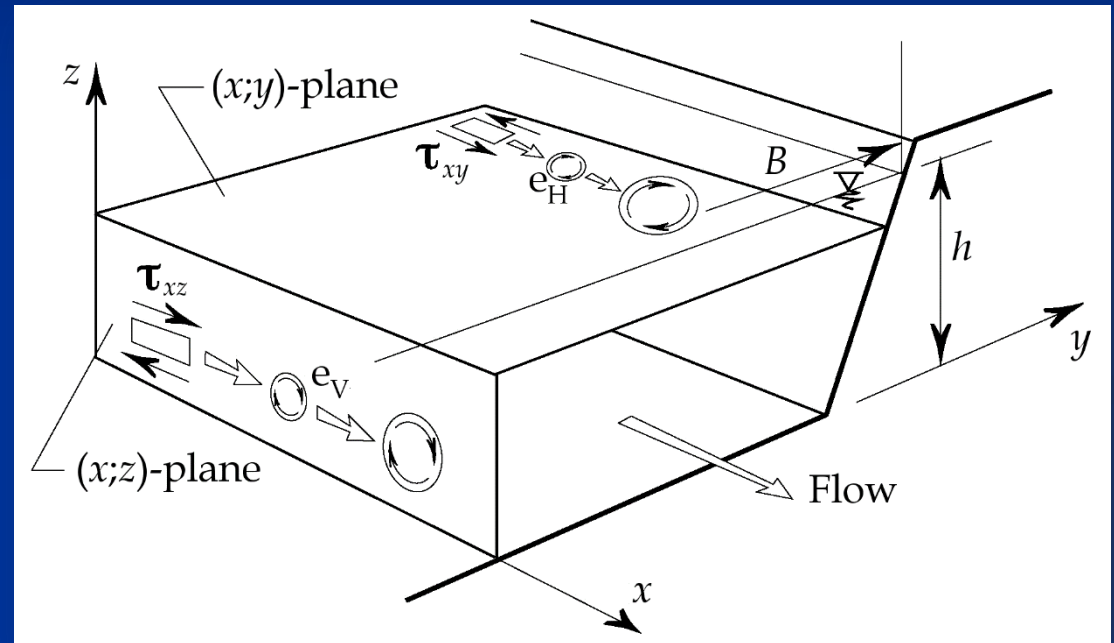
- **Large-scale coherent structures** (CS's) are the largest conglomeration of eddies which has a prevailing sense of rotation (Hussain, A.K.M.F. 1983, Phys. Fluids); **they scale with the external dimensions of the flow**



Cine-record due to Klaven 1966 showing an instantaneous view of large-scale CS's in an open-channel flow

# Vertical and Horizontal Coherent Structures

- CS's are “born” (with the “roll up” of an eddy), **grow** so as to eventually occupy the entire body of fluid, and finally disintegrate (i.e. “die”): Hussain 1983, Yalin 1992.



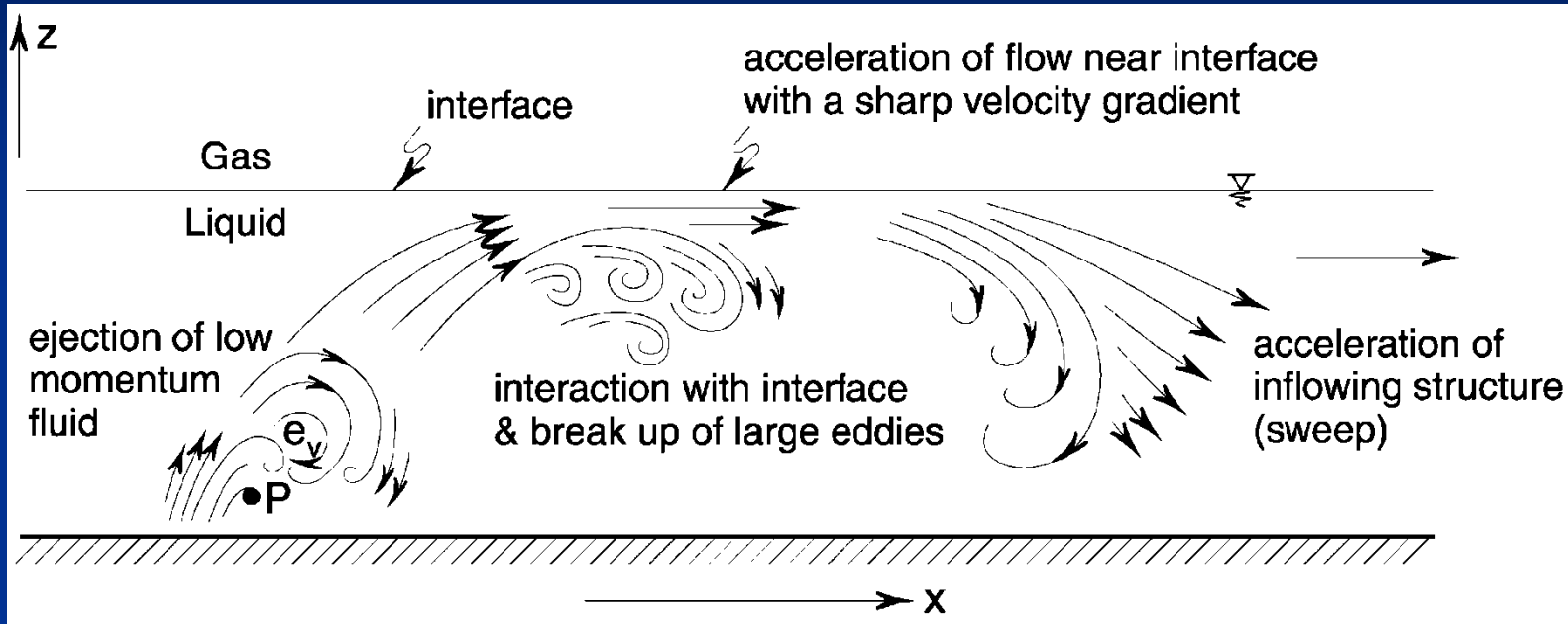
- In open-channel flows:*

Vertical CS's (VCS's):  $\mathcal{L} \sim h$

Horizontal CS's (HCS's):  $\mathcal{L} \sim B$

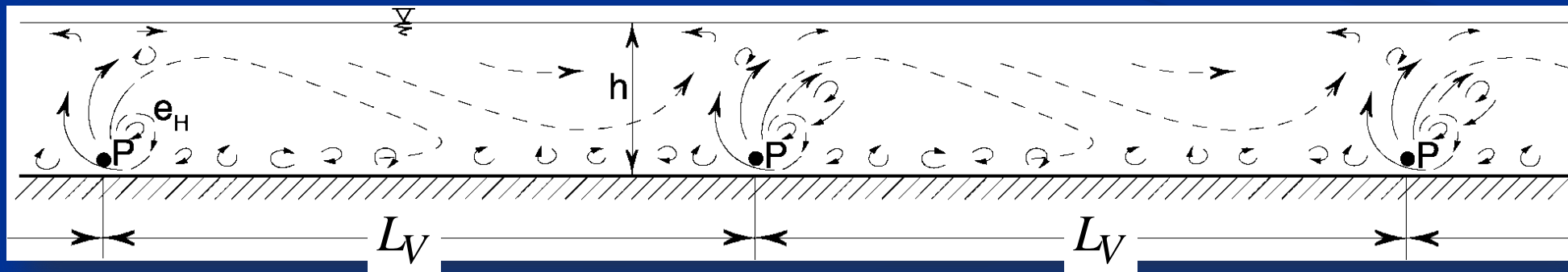
# Vertical CS's: sequence of events during a burst-cycle

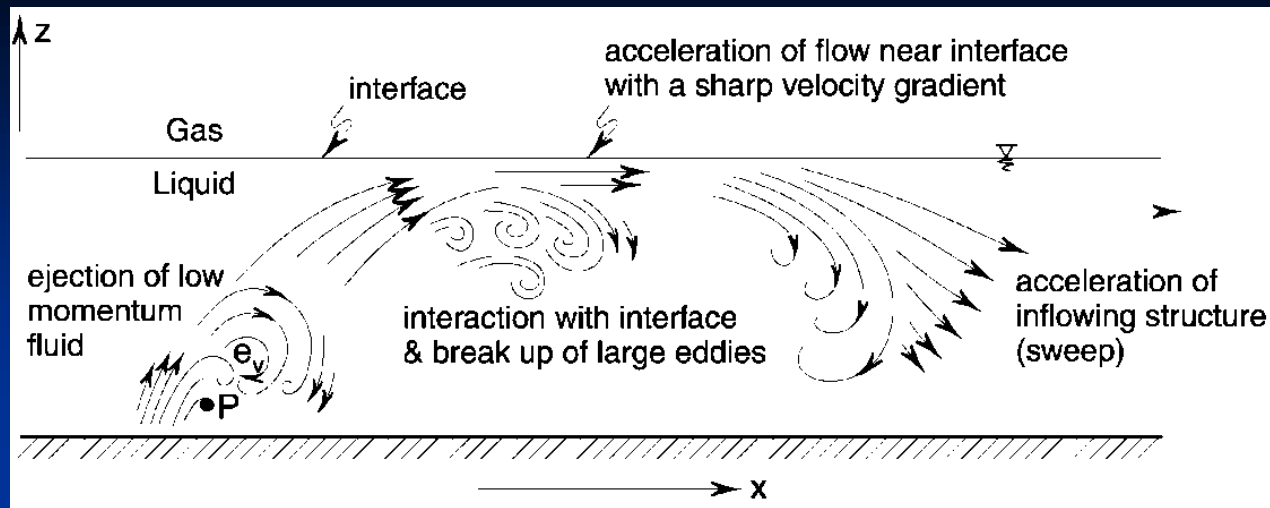
Synthesis based on: Blackwelder 1978, Cantwell 1981, Hussain 1983, etc.



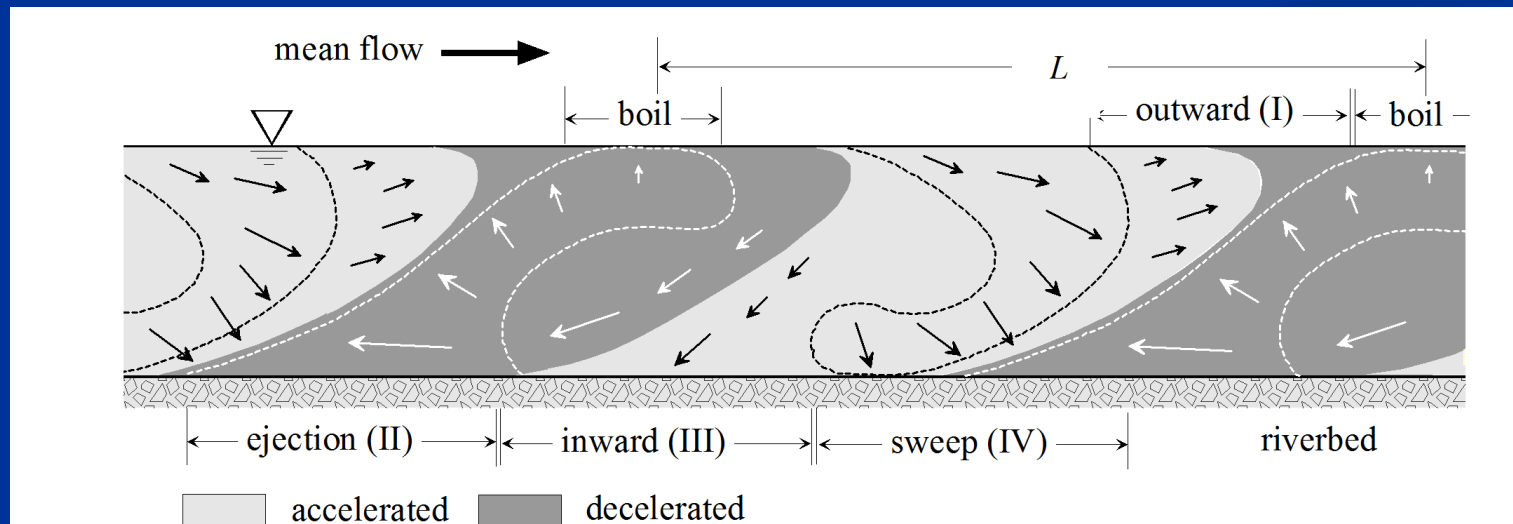
$$L_V = \text{Length scale}$$
$$T_V = \text{Timescale}$$
$$(\text{=} L_V / v)$$

Longitudinal view of flow (from da Silva 2006, J. Hydr. Res.)





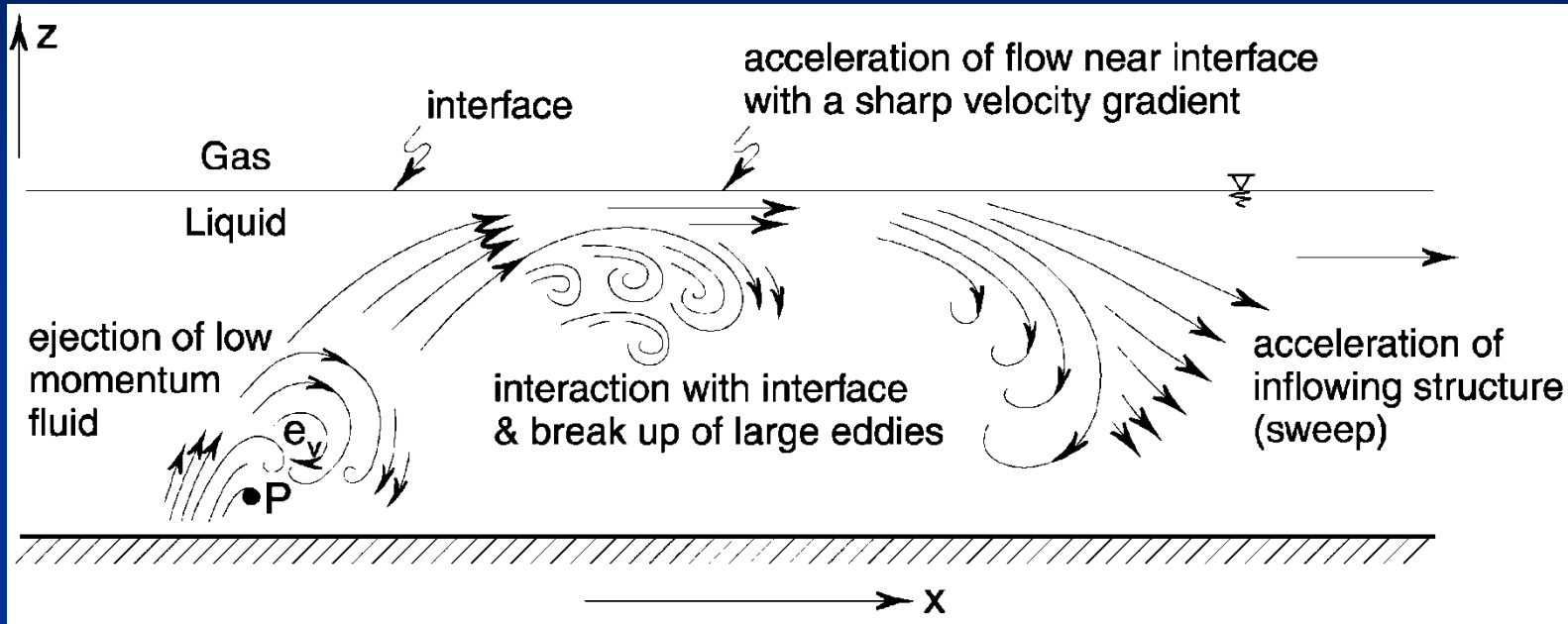
Longitudinal view of flow (from da Silva 2006, J. Hydr. Res.)



Longitudinal view of flow (from Sukhodolov 2011, J. Hydr. Res.)

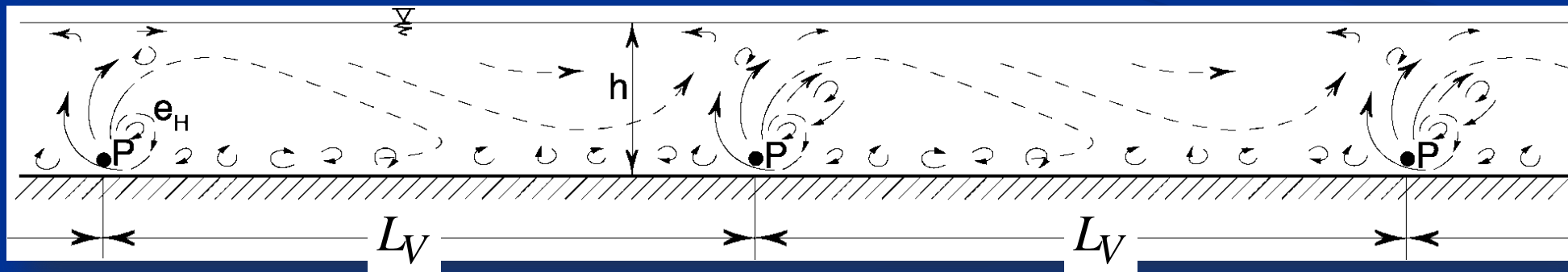
# Vertical CS's: sequence of events during a burst-cycle

Synthesis based on: Blackwelder 1978, Cantwell 1981, Hussain 1983, etc.

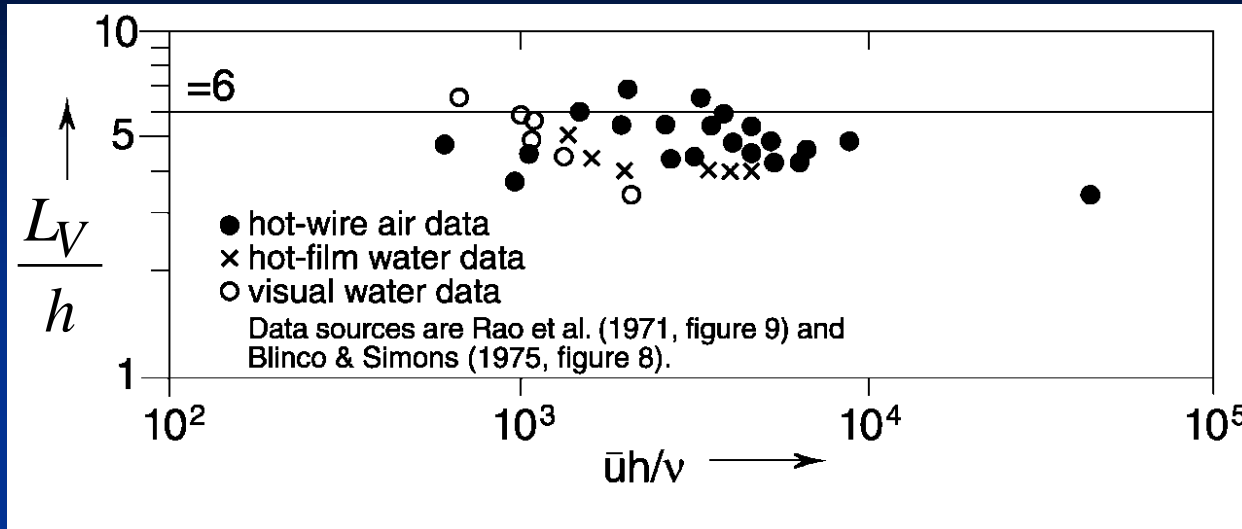


$$L_V = \text{Length scale}$$
$$T_V = \text{Timescale}$$
$$(\text{=} L_V / v)$$

Longitudinal view of flow (from da Silva 2006, J. Hydr. Res.)



# Vertical CS's: length scale

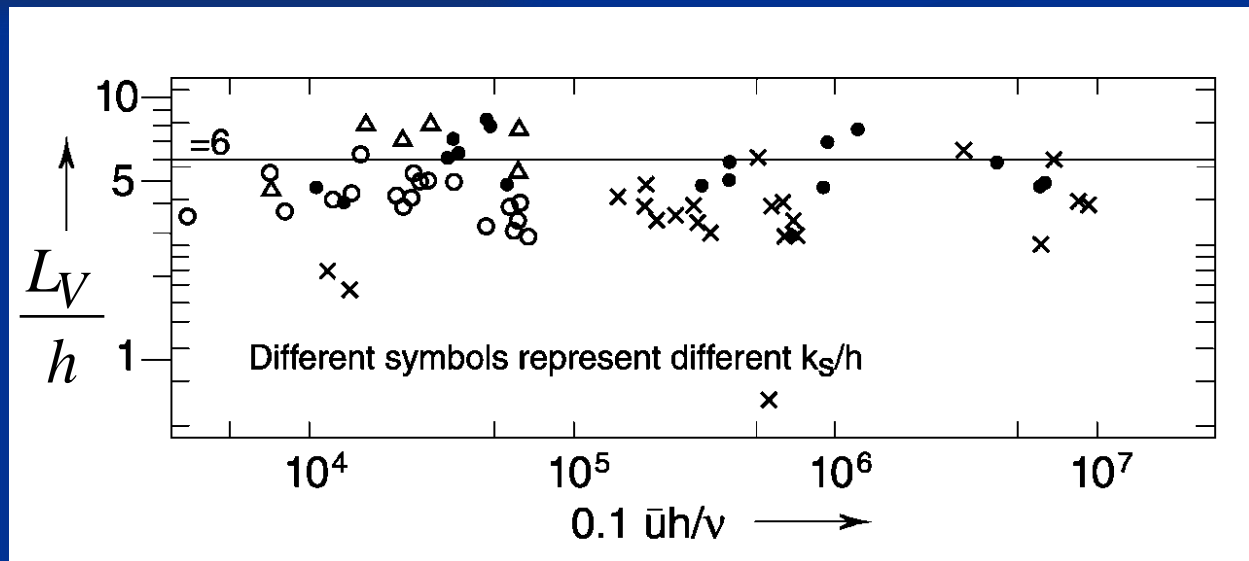


More recent measurements:

- Roy et al. 2004, J. Fluid Mech;
- Shvidchenko and Pender 2001, JHE
- Franca and Lemmin 2008, River Flow 2008

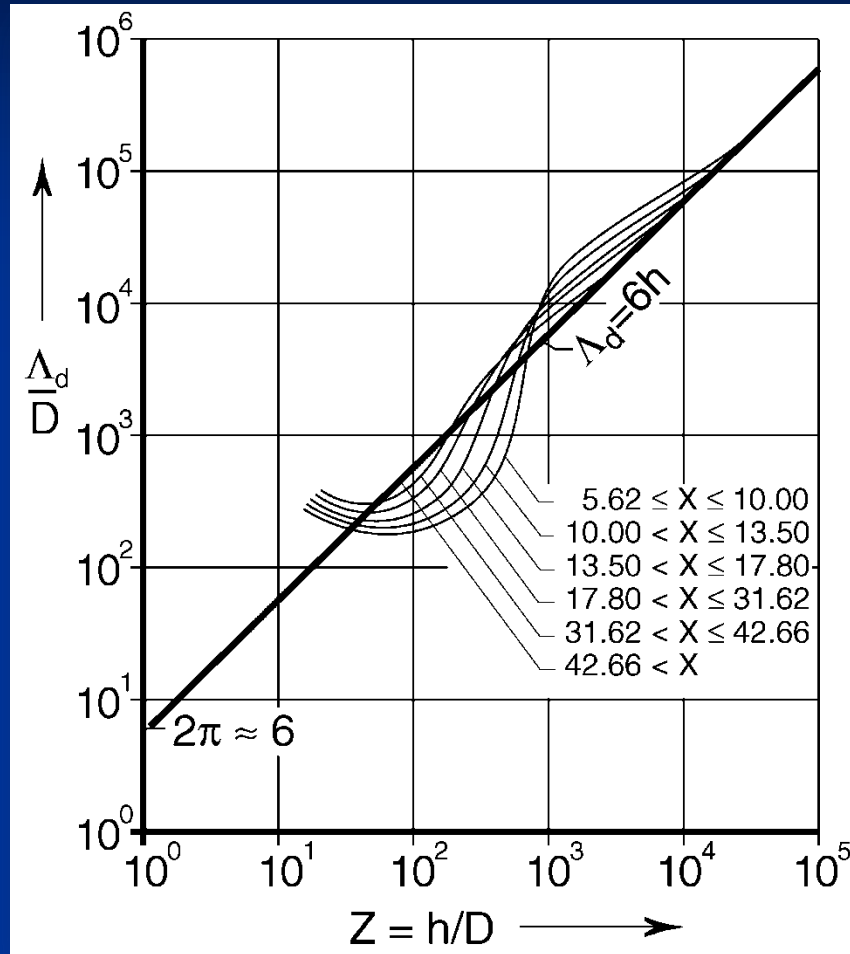
Earlier measurements  
(boundary-layer flows)

$$L_V \approx 6h$$



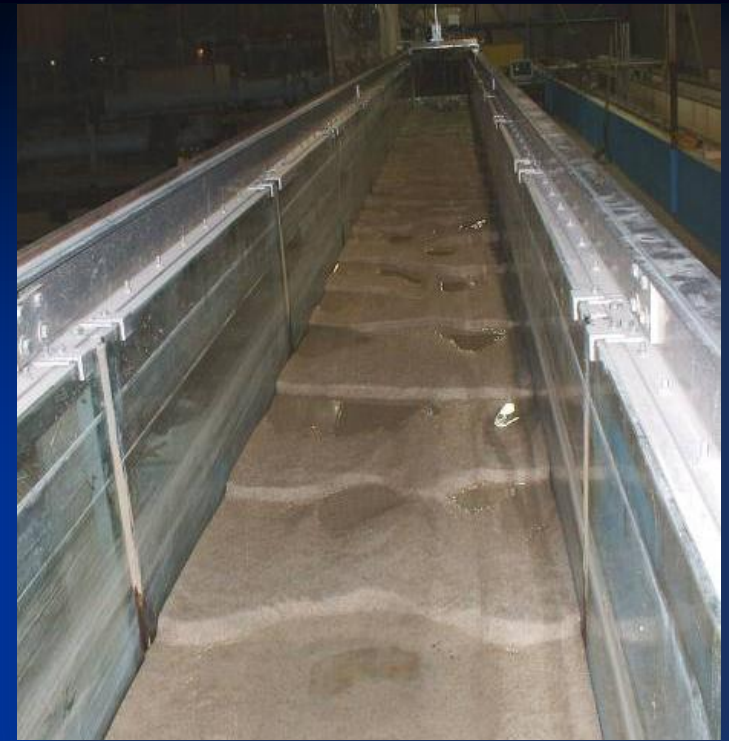
From Yalin 1992 (after Jackson 1976)

# Vertical CS's: morphological consequences

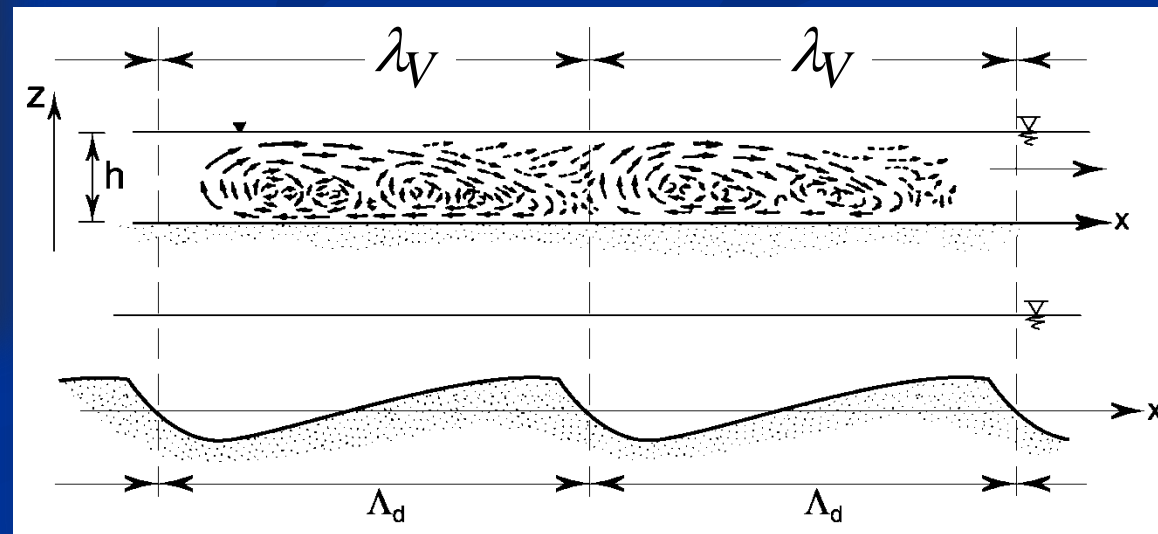


$$\Lambda_d \approx 6h$$

(Yalin 1977)



$$L_V \approx \Lambda_d \approx 6h$$





# Horizontal coherent structures (HCS's)

- In contrast to the case of large-scale vertical coherent structures, large-scale horizontal coherent structures (HCS's) have not yet been the focus of directed, systematic studies
- Yokosi 1967, Grishanin 1975, ...

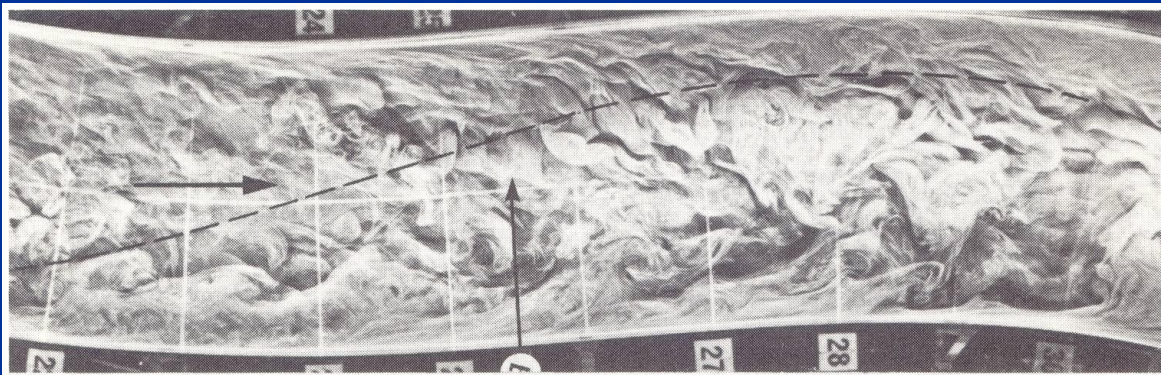
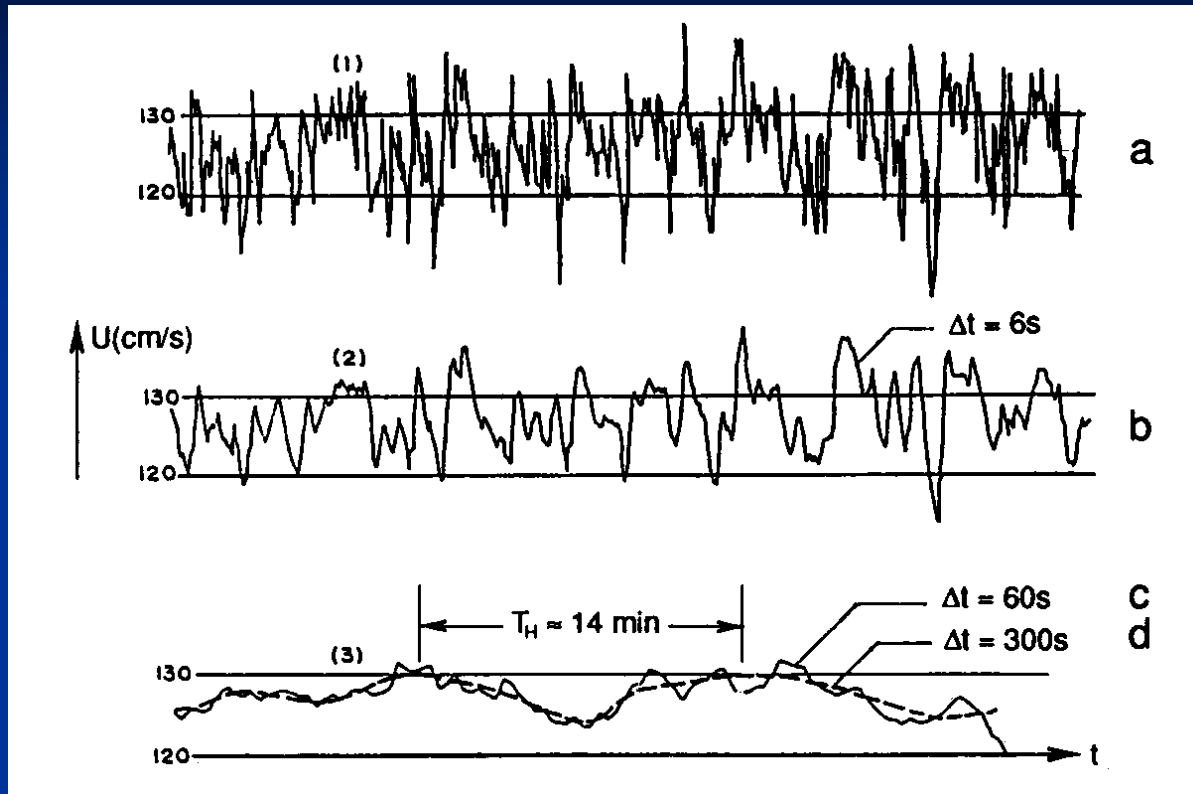


Photo by Prof. H. Ohnari, Tokuyama College of Technology; Top view of an open-channel flow

# Horizontal turbulence: burst length



$$T_H \approx 14 \text{ min}$$

$$\frac{L_H}{B} = \frac{v T_H}{B} =$$

$$= \frac{(1.10)(14)(60)}{100} = 9.24 \approx 9$$

From Yokosi 1967; Measurements in Uji River;  $B=100\text{m}$ ;  $v=1.10\text{m/s}$

Similar study in Syr-Darya River at Ak-Ajar by M.A. Dementiev 1962 and K.V. Grishanin 1979:

$$L_H / B \approx 7$$

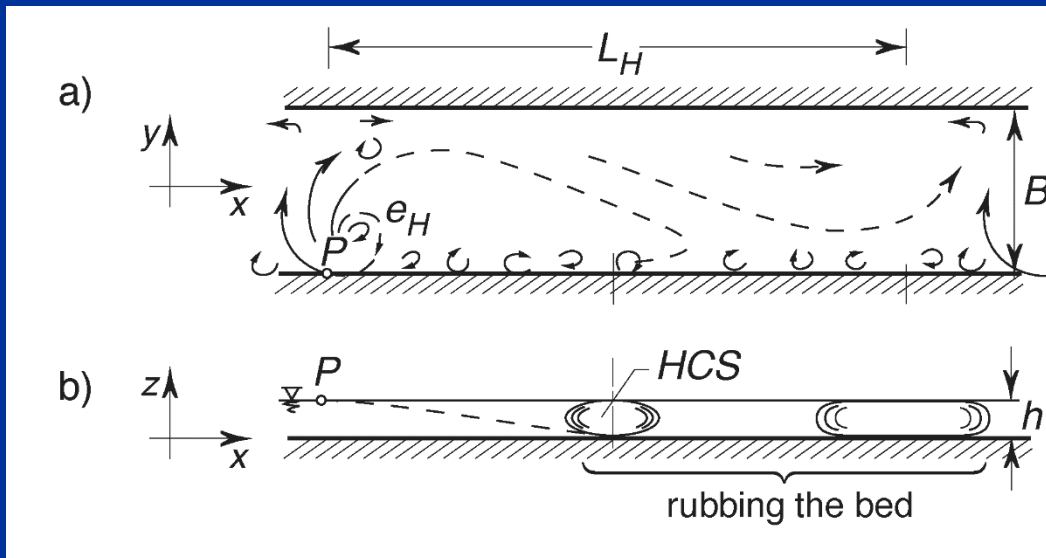
# The turbulence-based explanation for the origin of alternate bars of Yalin and da Silva (2001)

$L_H =$  Length scale  $\sim B$

$T_H =$  Time scale  $(= L_H / v)$

- In their life-cycle, HCS's follow a sequence of events similar to that followed by VCS's, with the difference that they occur in a horizontal "flow ribbon" (Yalin 1992, "River Mechanics")

Difference: length scale

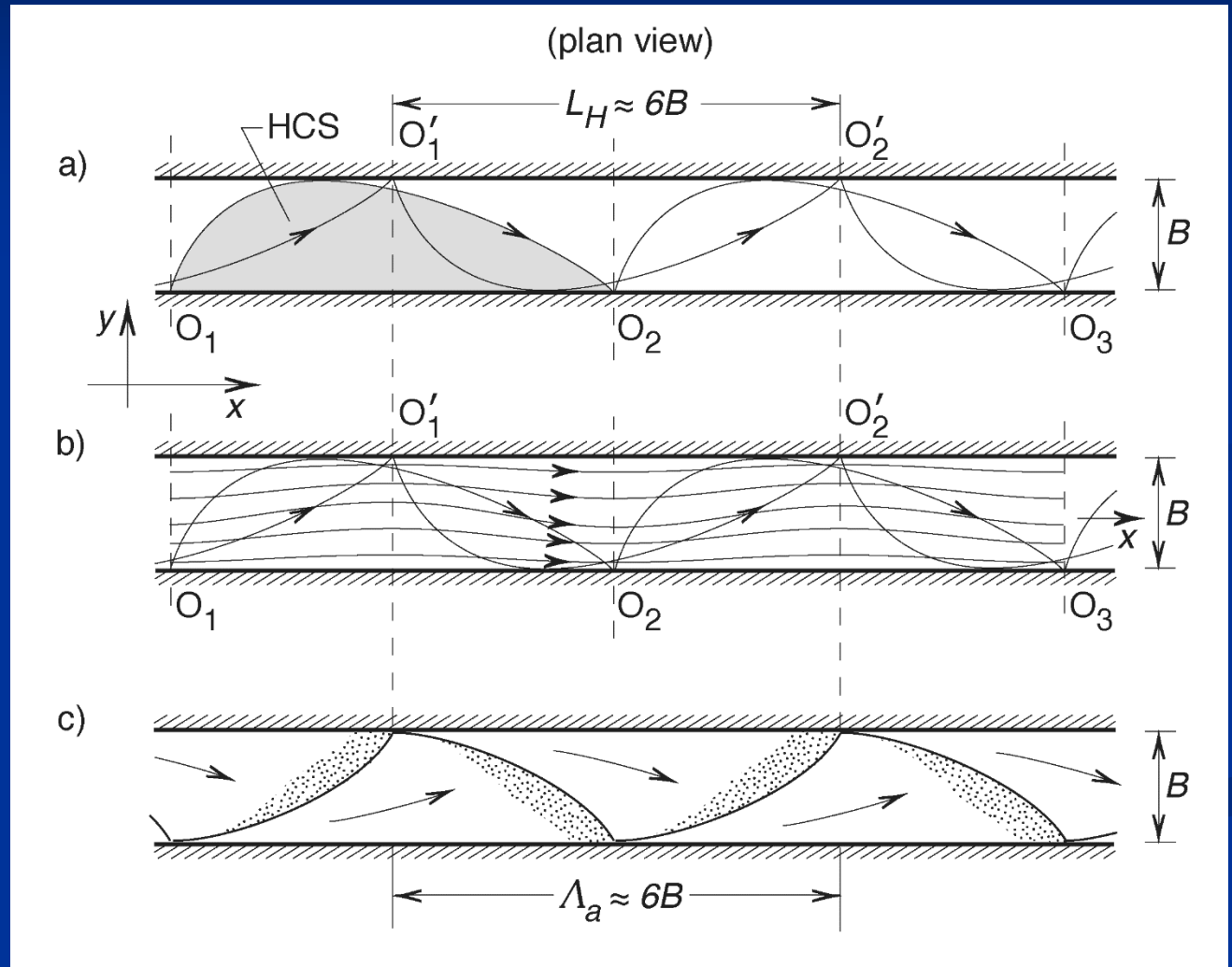


Plan View

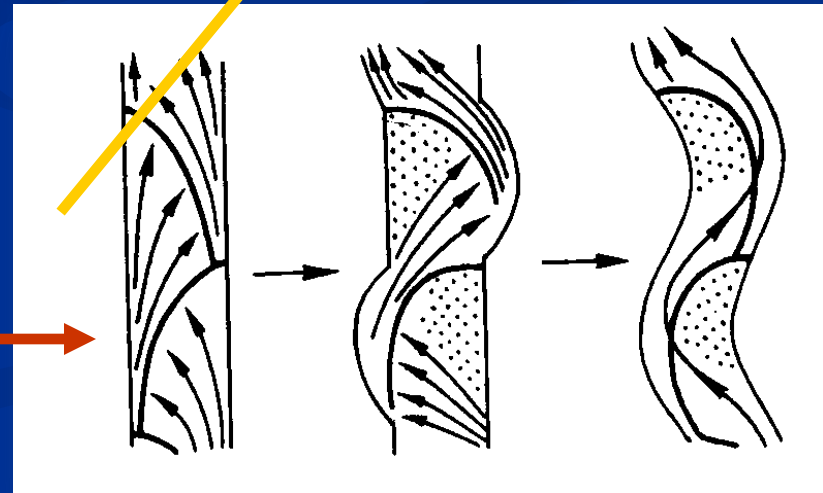
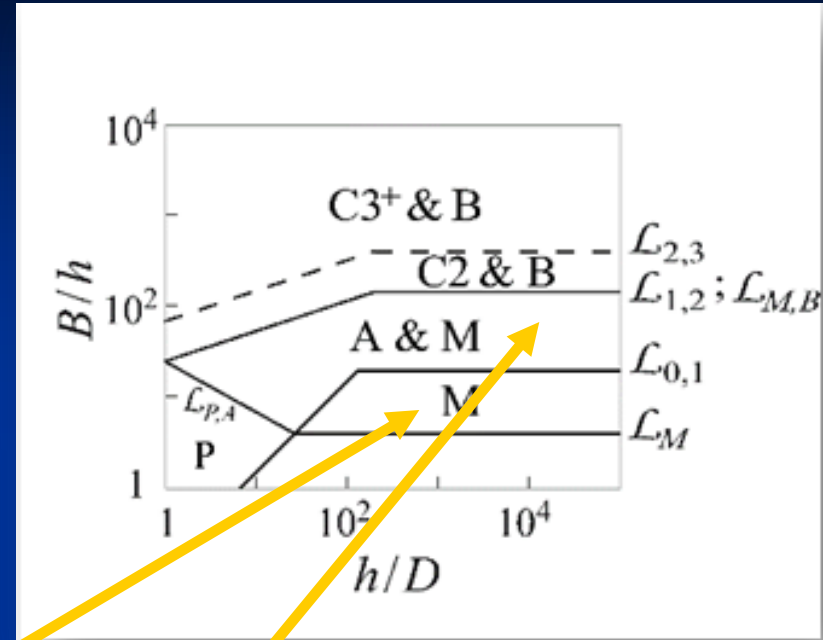
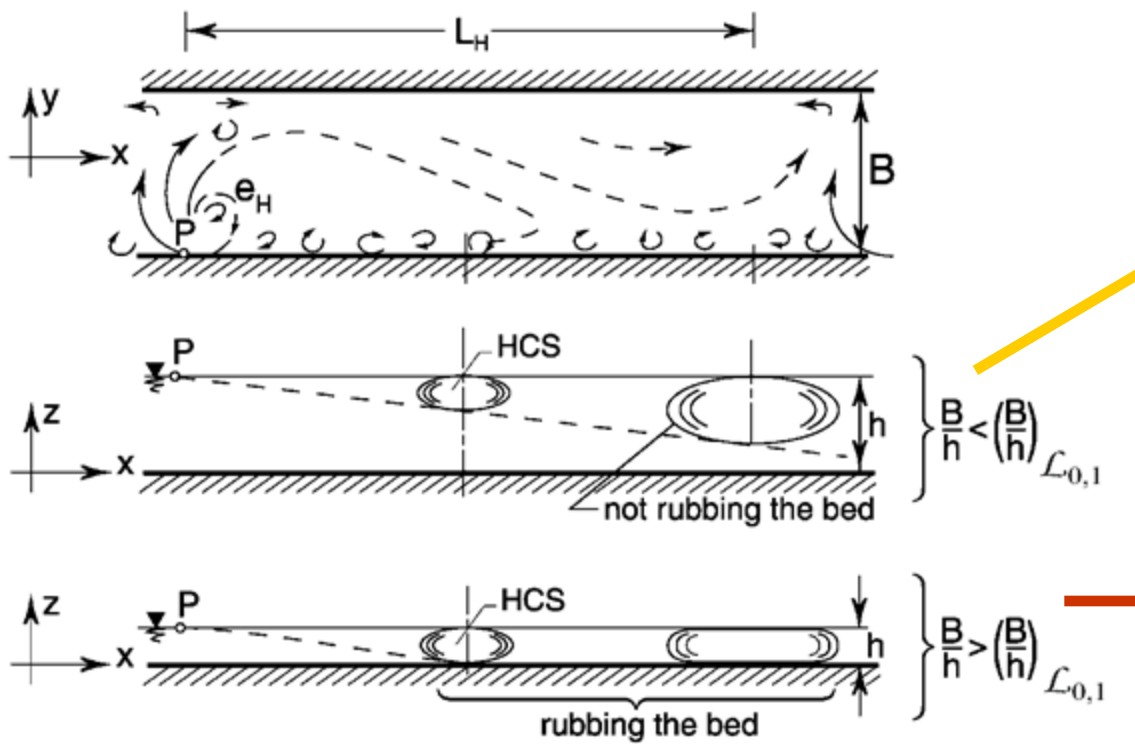
Side View

Disks (Yokosi 1967, Jirka and Uijttewaal 2004)

# The turbulence-based explanation for the origin of alternate bars (Yalin and da Silva (2001))



# The turbulence-based explanation for the origin of alternate bars of Yalin and da Silva (2001)



# Experimental Set-up

## Channel:

- 1 m-wide
  - 21 m-long
  - 0.4 m-deep
- 
- Bed formed by sand having  $D_{50}=2\text{mm}$ ; Flat bed surface



# Flow conditions

( $B/h; h/D$ ) – plan of Yalin and da Silva 2001;  
Existence region plan of alternate bars

$$Q = 34.4 \text{ l/s}$$

$$B = 1 \text{ m}$$

$$D = 2 \text{ mm}$$

$$h = 14 \text{ cm}$$

$$S_0 = 0.0005$$

$$S_f = 0.00027$$

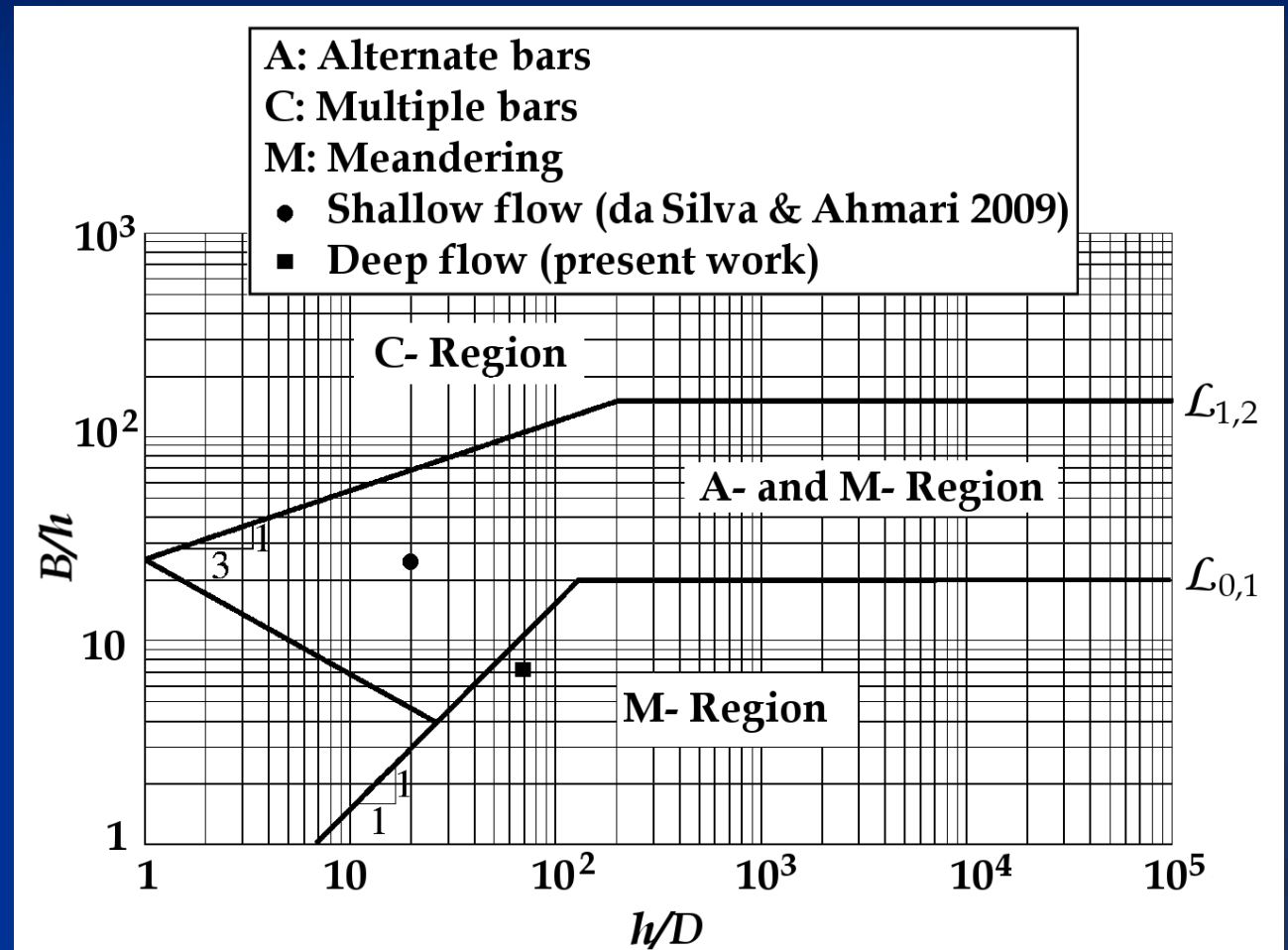
$$v = 24.5 \text{ cm/s}$$

$$Fr = 0.2$$

$$Re = 34300$$

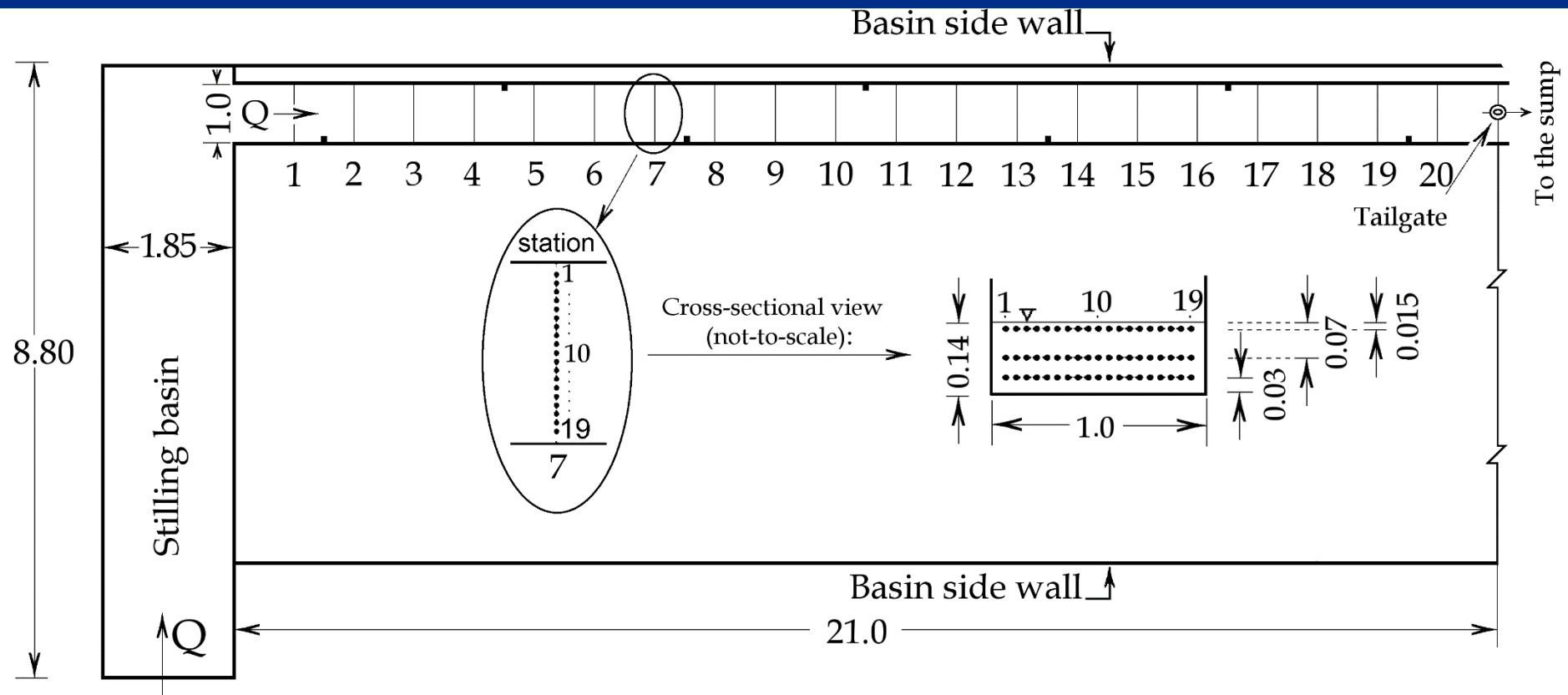
$$Re_* = 64.8$$

$$Y/Y_{cr} = 0.18$$



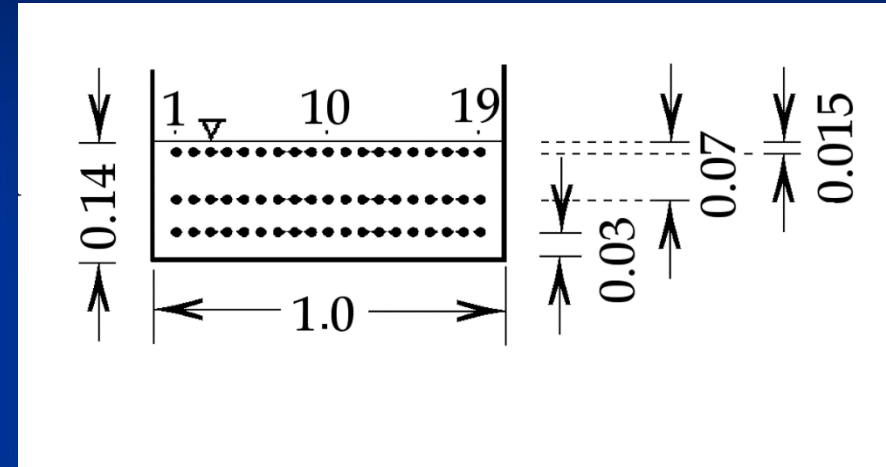
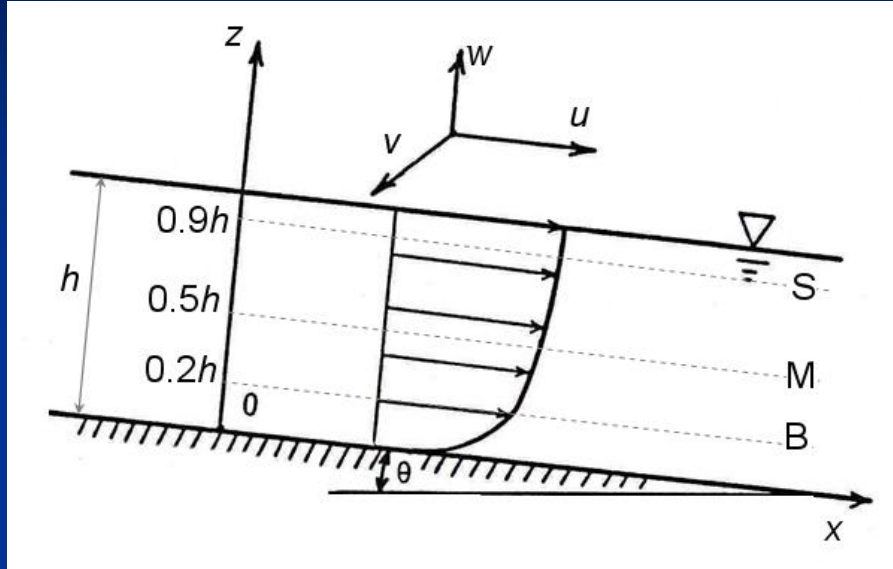
Deep flow:  $B/h=7$  ;  $h/D=70$

# Deep flow: flow measurements





# Flow measurements

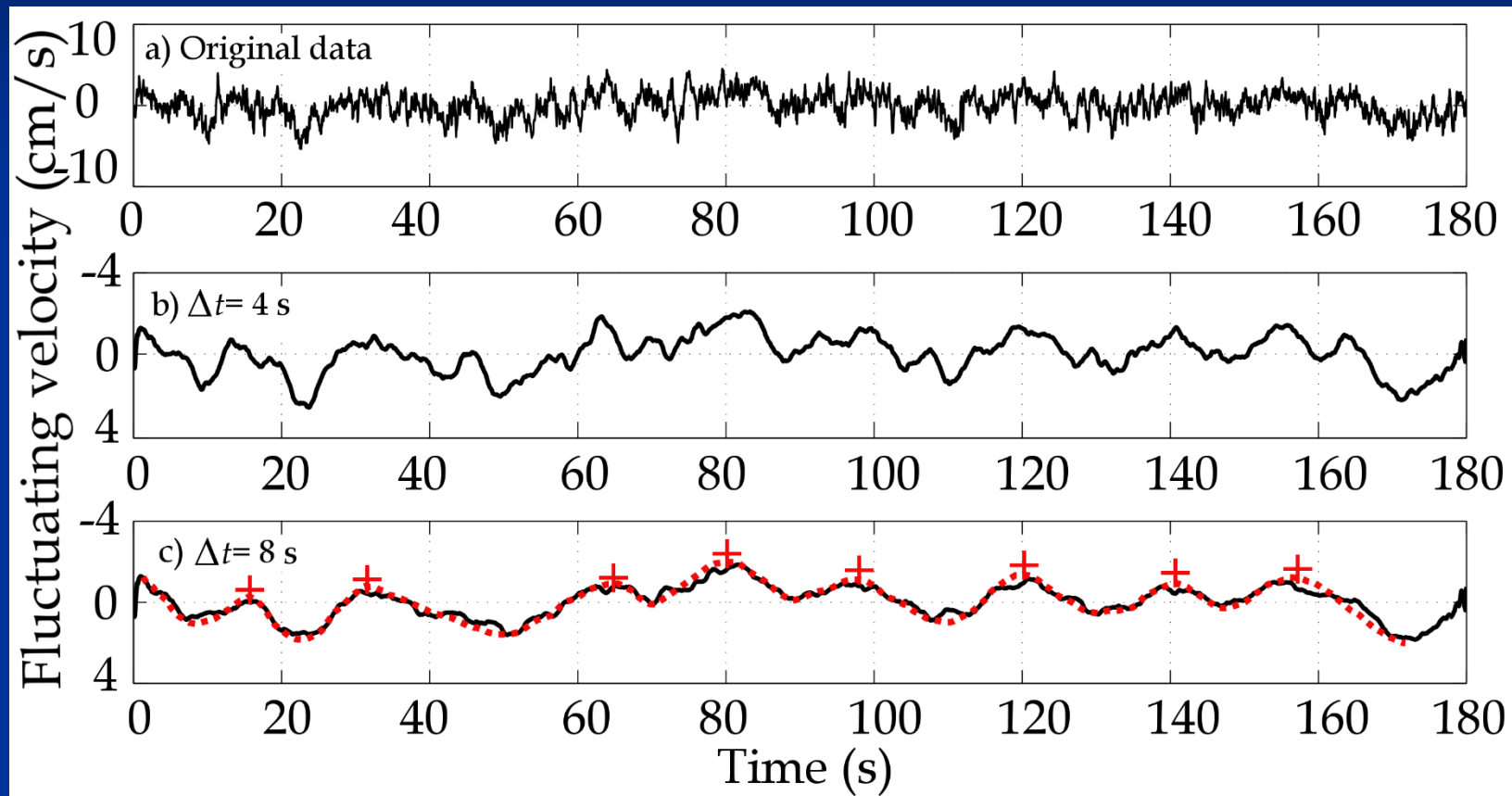


- **16-MHz 2D Son TeK™**
- **Frequency of sampling: 25 Hz**
- **Duration of measurements: 180 s; 20 min at selected stations**



## Results for $z/h = 0.9$

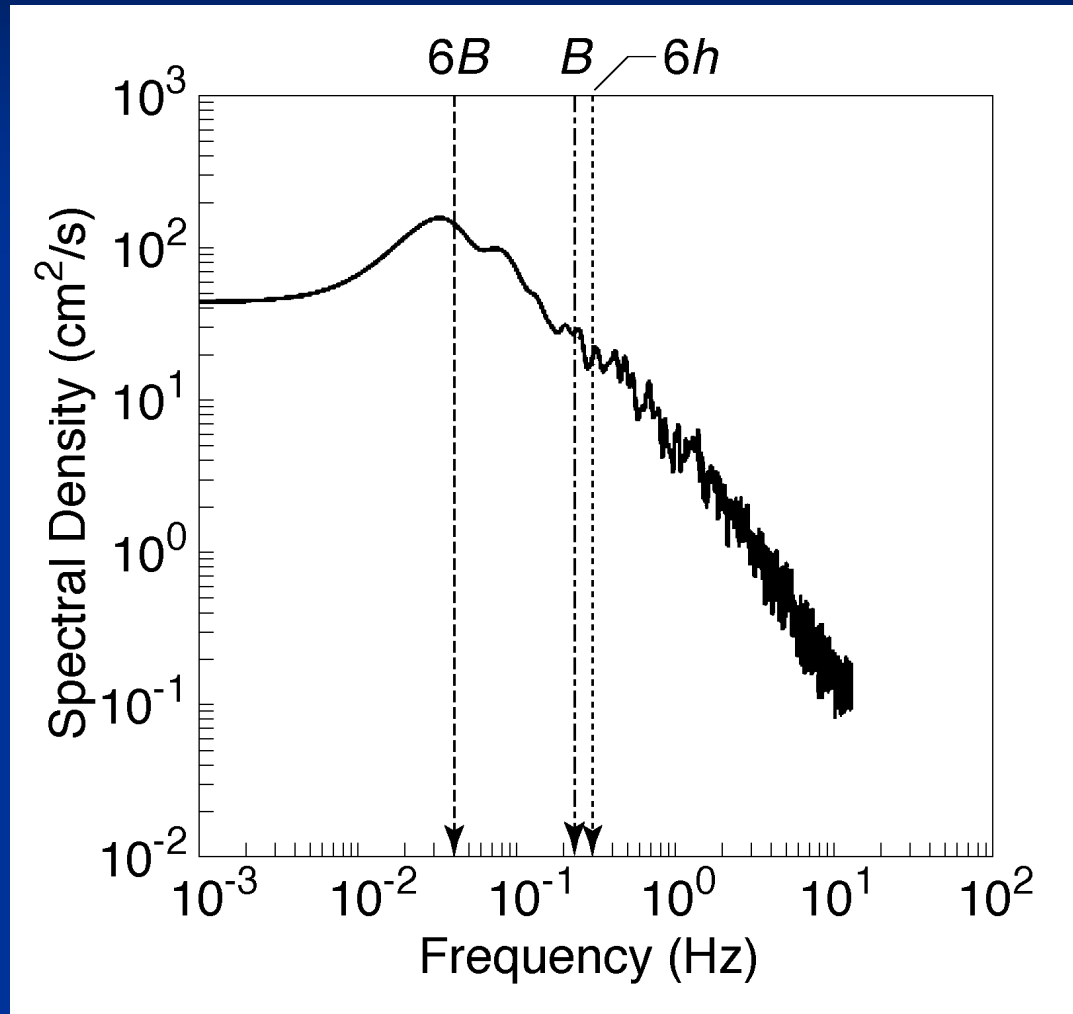
### i) Smoothing (filtering) of the oscillograms of the fluctuating component of longitudinal velocity



- Sample of application of moving average filter on fluctuating velocity record at the level  $z/h \approx 0.9$  (section 10, station 10)  
 $T_H = (160 - 15) / 7 = 20$  s or  $L_H = 20 \times 0.245 = 5$  m =  $5B$

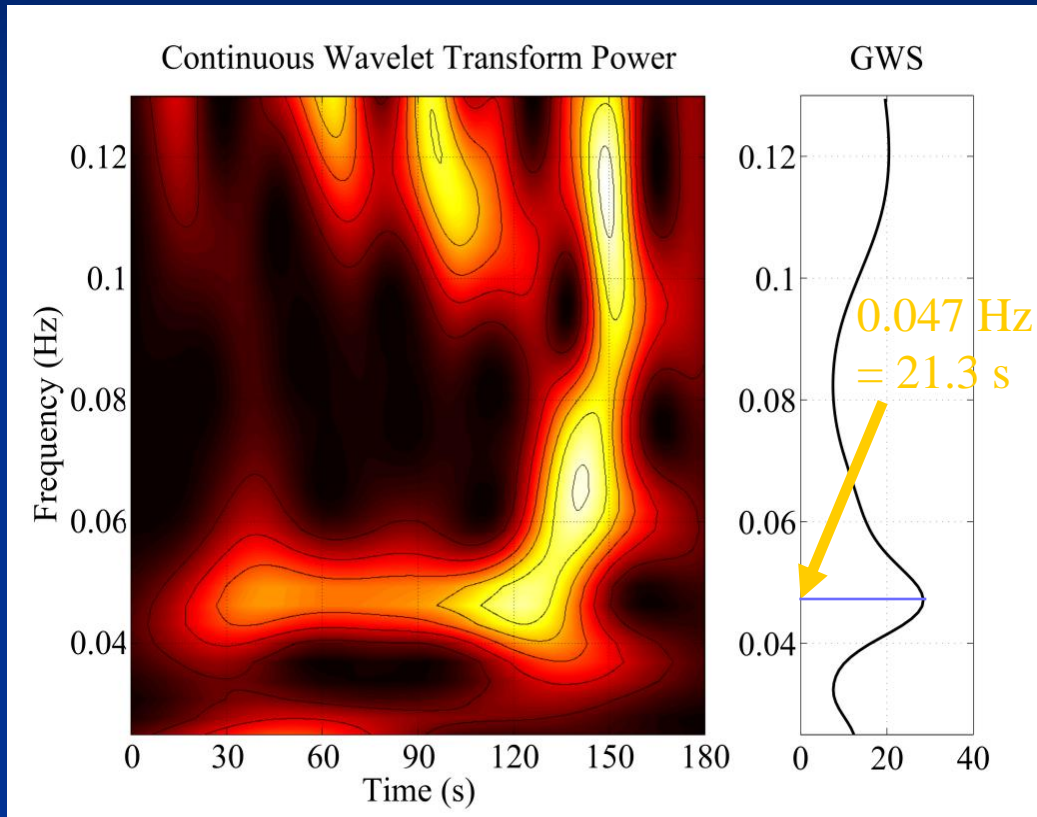
# Results for $z/h = 0.9$

## ii) Energy spectrum



# Results for $z/h = 0.9$

## iii) Continuous wavelet transform

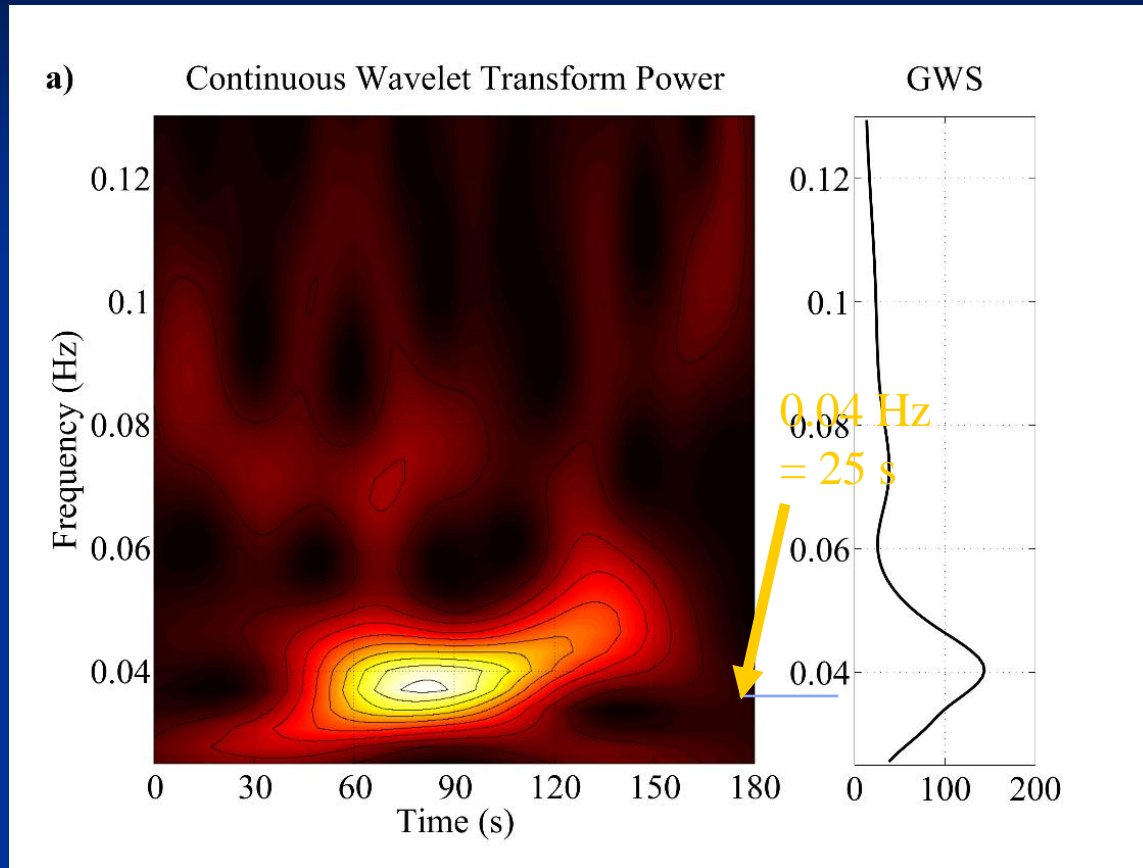


Sample of application of continuous wavelet transform to the fluctuating velocity record at section 10, station 2

Continuous Wavelet Transform (CWT) is a powerful tool for the identification and scale characterization of coherent structures in open channel flows (Camussi, 2002; Franca and Lemmin, 2006).

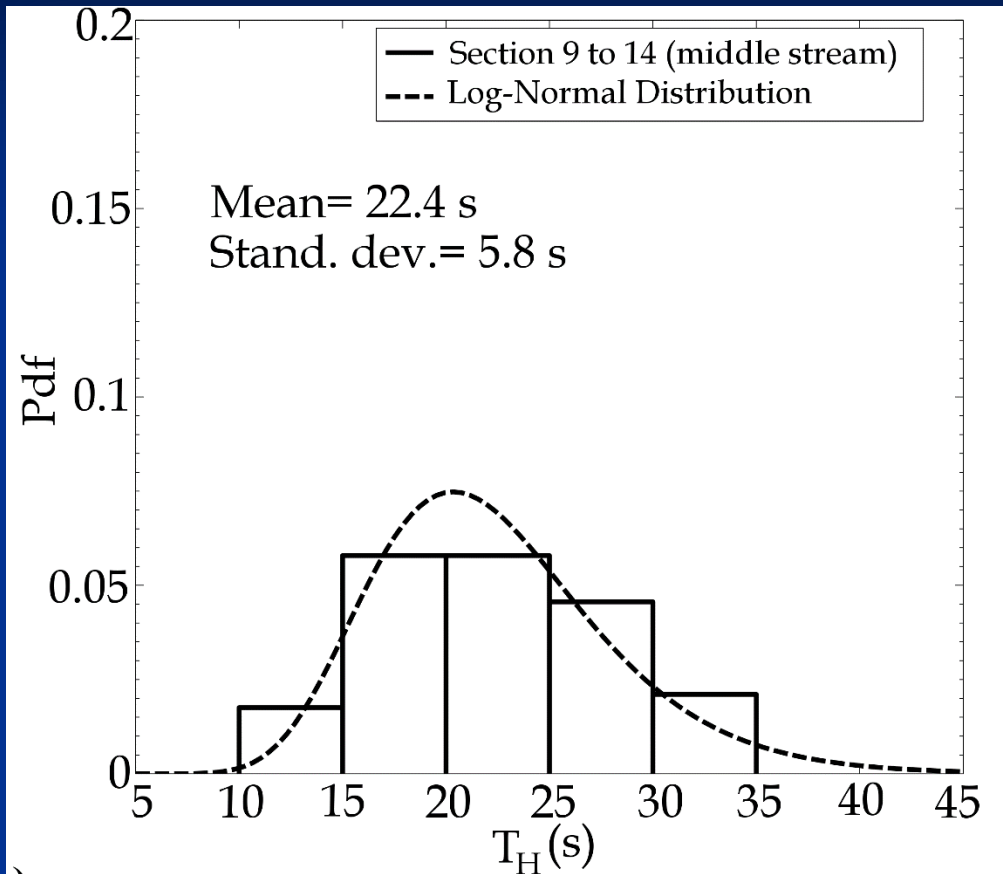
The method is particularly suitable for non-stationary signals, yielding both the frequency components of a signal, as well as the time localization of the frequency components of the signal.

# Results for $z/h = 0.9$



Sample of application of continuous wavelet transform to the fluctuating velocity record at section 9, station 12

# Time and length scales



The probability distribution function (Pdf) of horizontal burst-period resulting from the application of the just described procedure to the set of 3 min long velocity records collected at  $z/h=0.9$  (sections 9 to 14). The dashed line in this figure is the fitted log-normal distribution.

$$T_H \approx 22.4s$$

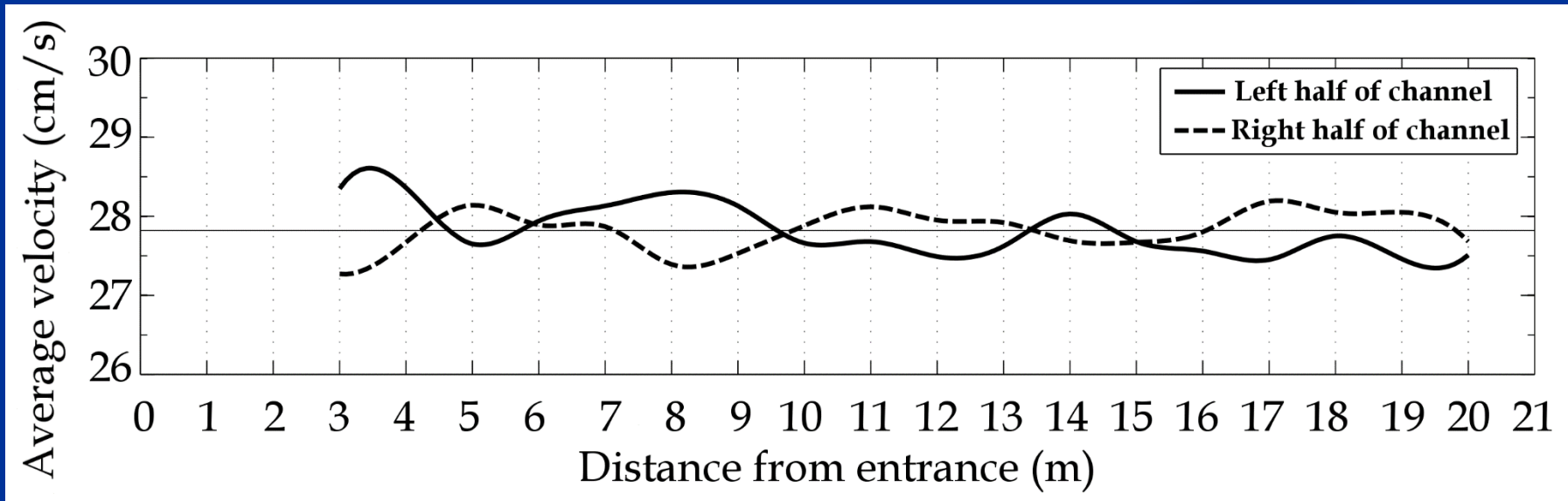
$$T_H / B = v \cdot T_H / B = 0.245 \times 22.4 / 1 = 5.5$$

# Results for $z/h = 0.9$

## Effect of HCS's on the mean flow

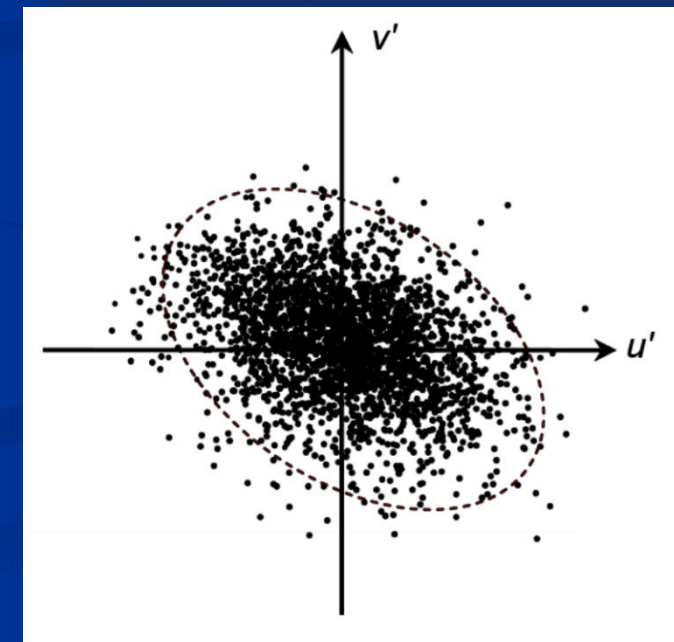
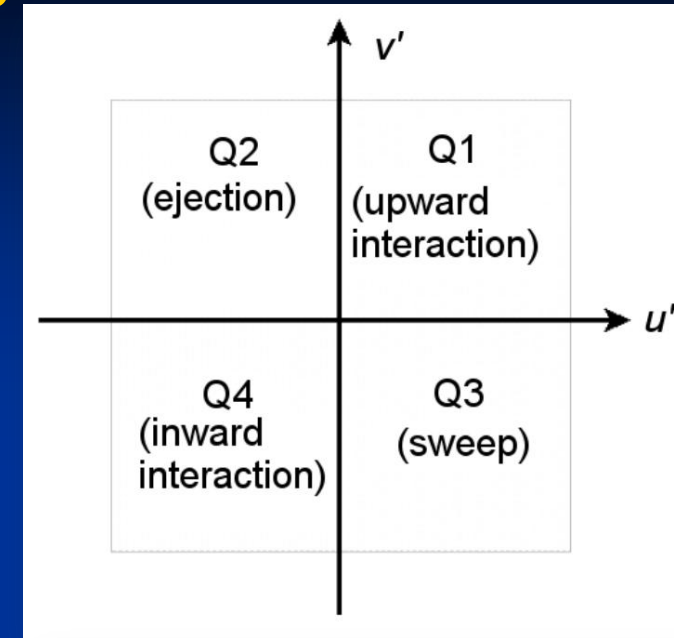
- Time-averaged Flow Velocity

The average flow velocity at the level  $z/h \approx 0.9$  for the left and right halves of the channel. The pattern is consistent with the existence of an internal meandering of the flow. This pattern is also consistent with previous findings for the case of a shallow flow.



# Deep flow results: Quadrant Analysis

- In open-channel flows, quadrant analysis is used to study the joint behaviour of the longitudinal and vertical fluctuating velocities to investigate the bursting phenomena of VCS's (Nakagawa and Nezu 1993, Buffin-Belanger et al. 2000, Maltese et al. 2007).
- Ahmari (2010), whose study is believed to be the first application of quadrant analysis to the detection of HCS's in open-channel flows, used this technique to investigate the existence of HCS's.
- Ejection ( $u' < 0, v' > 0$ ); Sweep ( $u' > 0, v' < 0$ ); Upward interaction ( $u' > 0, v' > 0$ ); Inward interaction ( $u' < 0, v' < 0$ )

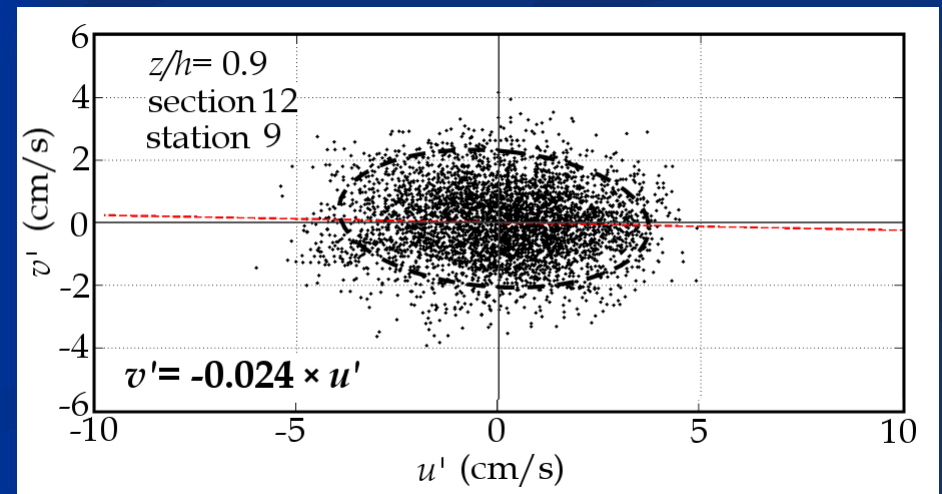
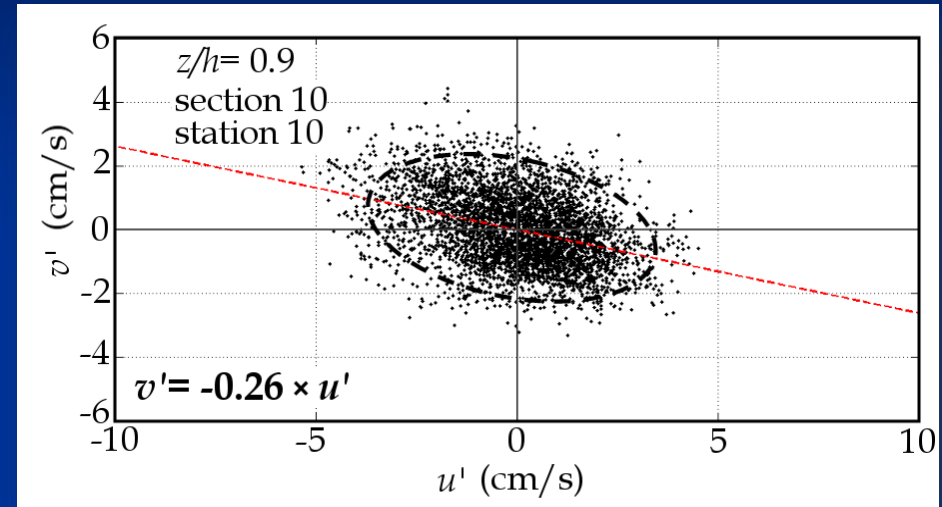




# Deep flow results: Variation of flow structure over the flow depth

## Coherent structures existence index (CSEI)

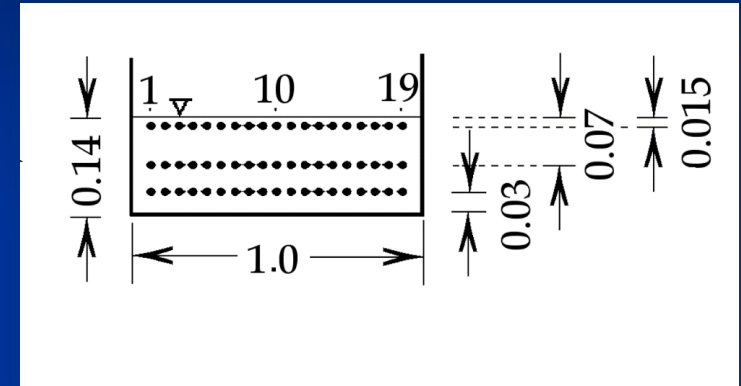
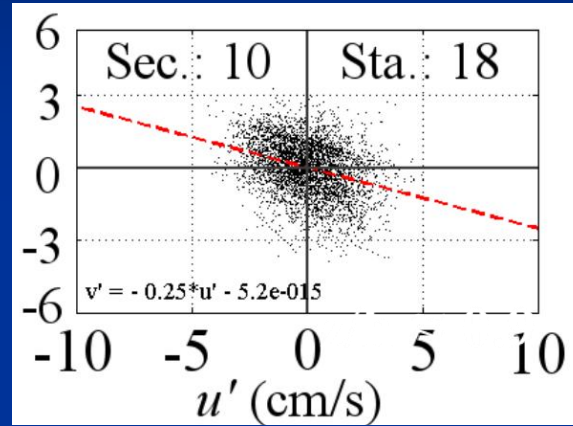
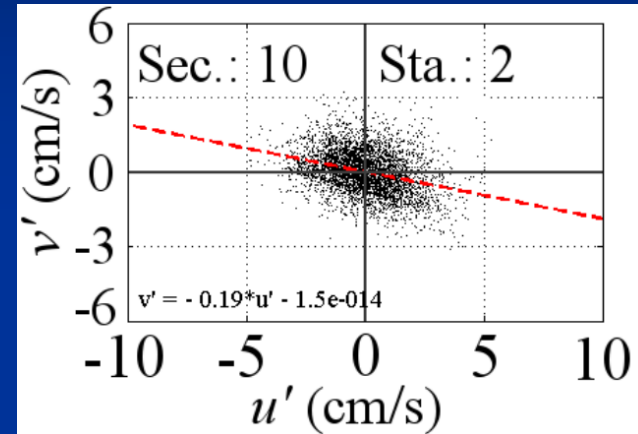
- If the major axis (or transverse diameter) of the hypothetical ellipse representing the data on the quadrant planes exhibits a slope, then that implies the more frequent occurrence of specific events related to coherent structures out of the four following possibilities.
- when the slope approaches to zero the data are almost evenly distributed in all quadrants, then that either reflects a large influence of flow structures associated with opposite shear layers, or incoherent background flow structures.



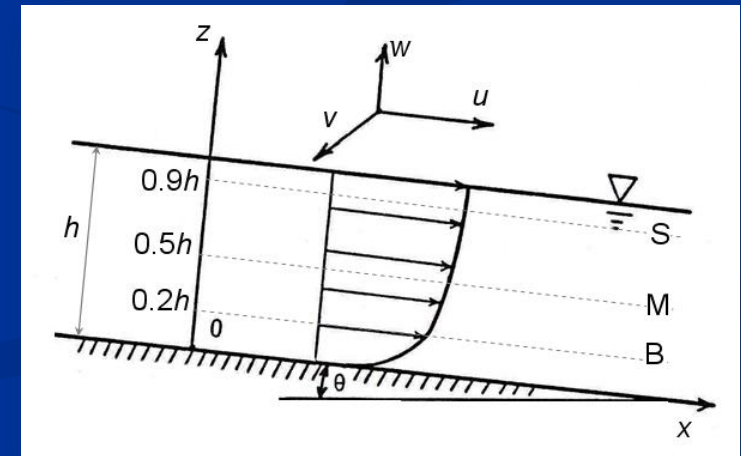
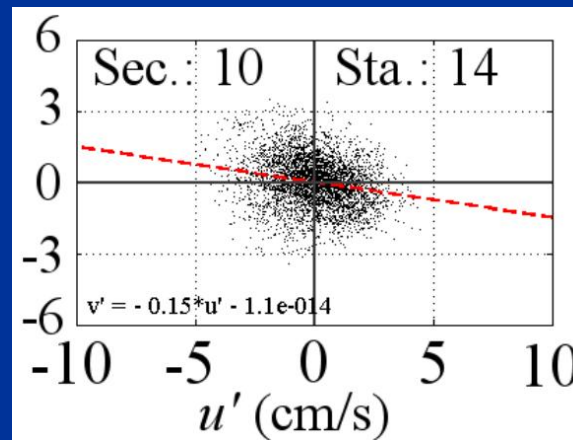
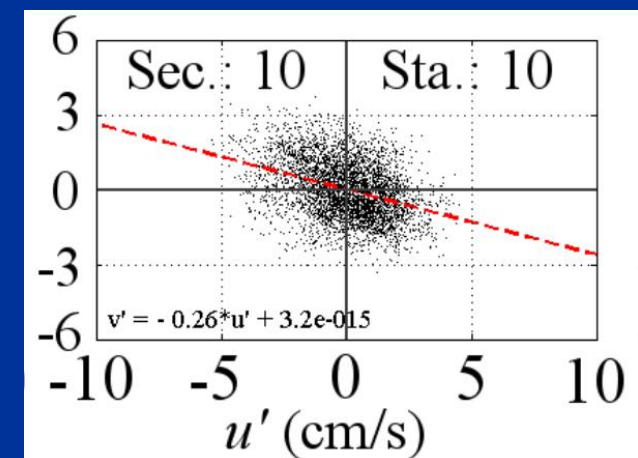
# Results for $z/h = 0.9$

## Quadrant Analysis

Near the banks:



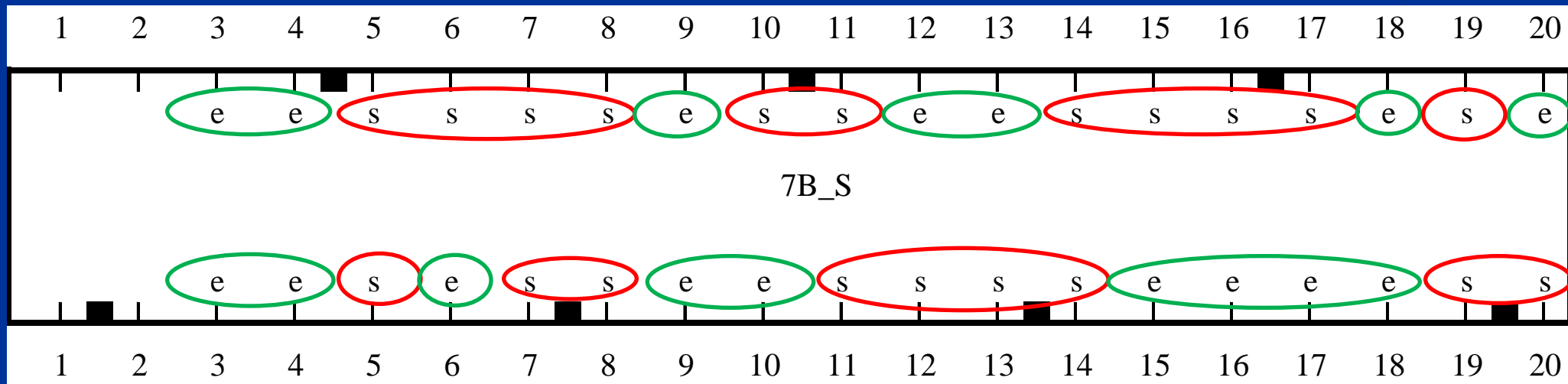
Centreline region:



# Quadrant Analysis

- The probability of occurrence of Q2 and Q4 events was different depending on the location in the flow field. At some locations, there was an increased probability of occurrence of ejection events, while at others an increased probability of sweep events

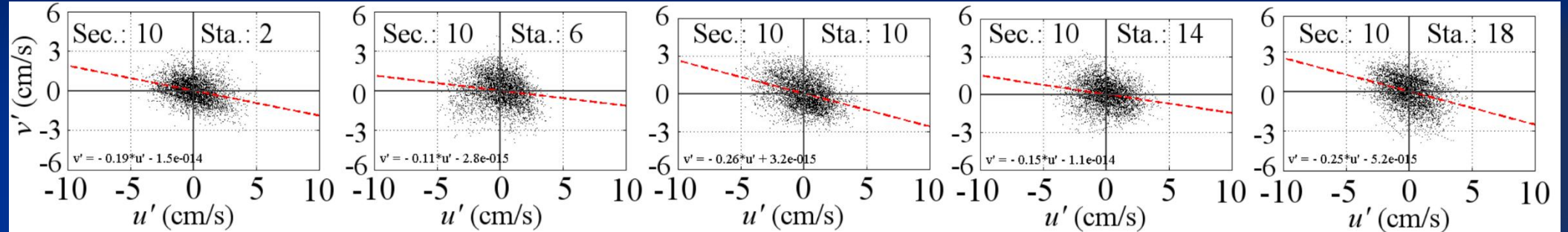
## Preferential locations of ejection and sweep events:



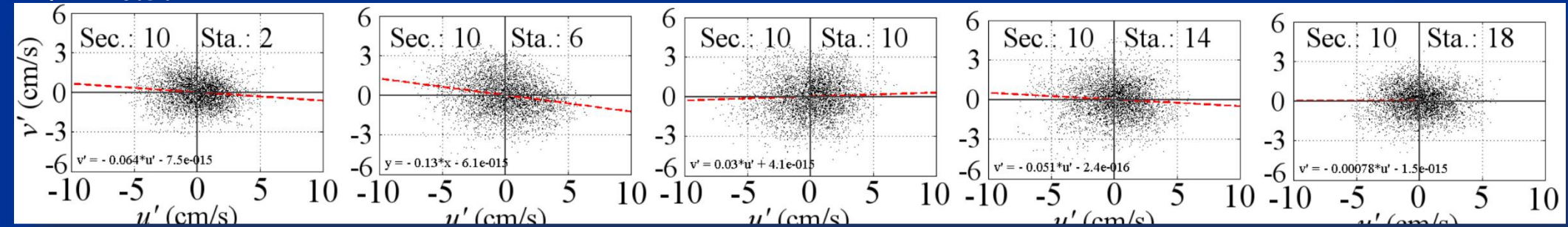
e = ejection; s = sweep; ■ blocks

# Variation of flow structure over the flow depth

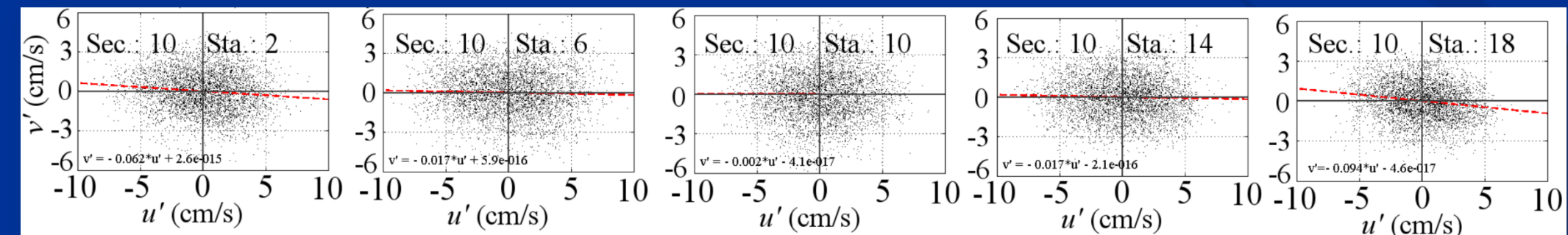
$z/h \approx 0.9$ :



$z/h \approx 0.5$ :



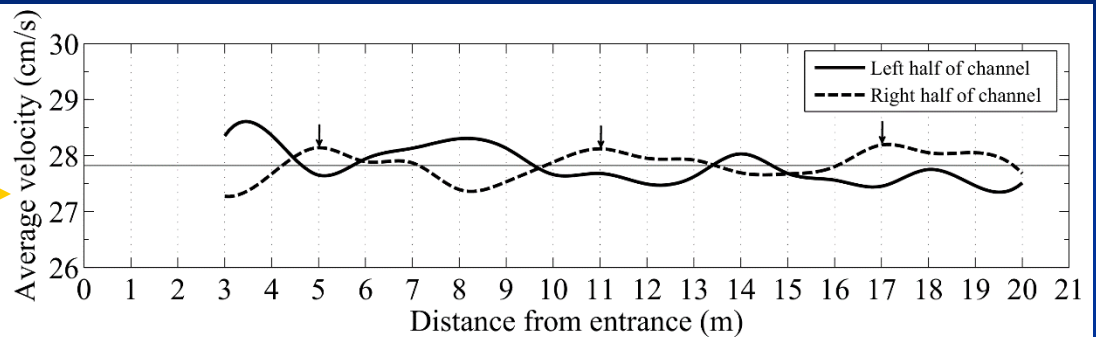
$z/h \approx 0.2$ :



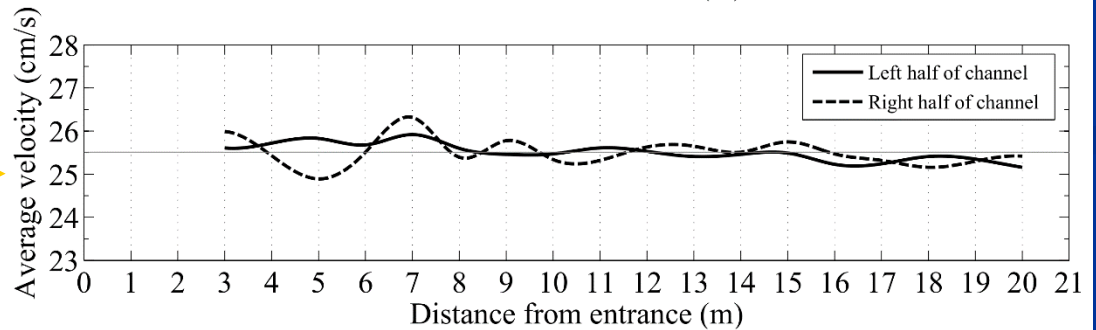
# Effect of HCS's on the mean flow over the flow depth

## • Time-averaged Flow Velocity

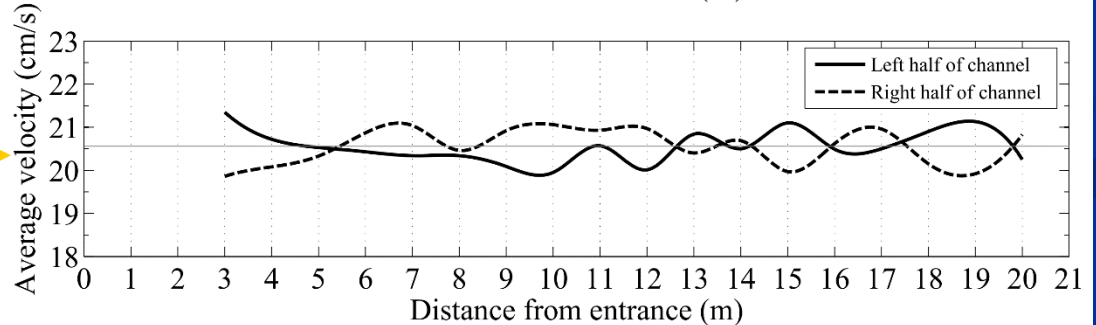
$z/h \approx 0.9$



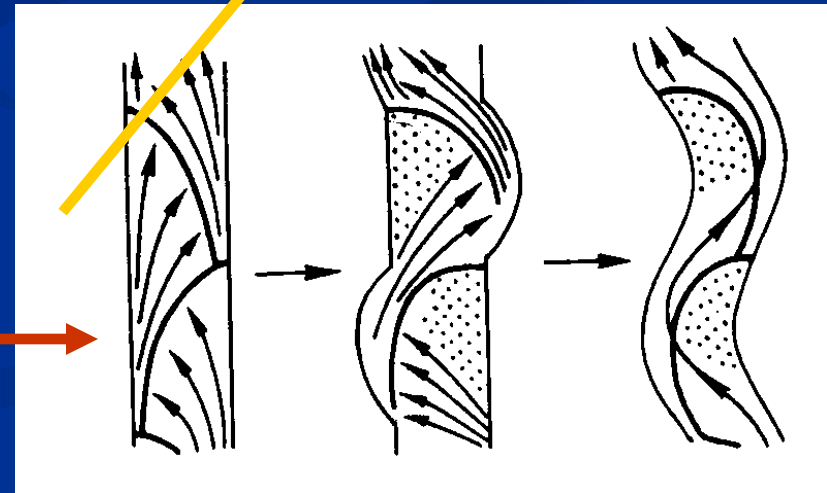
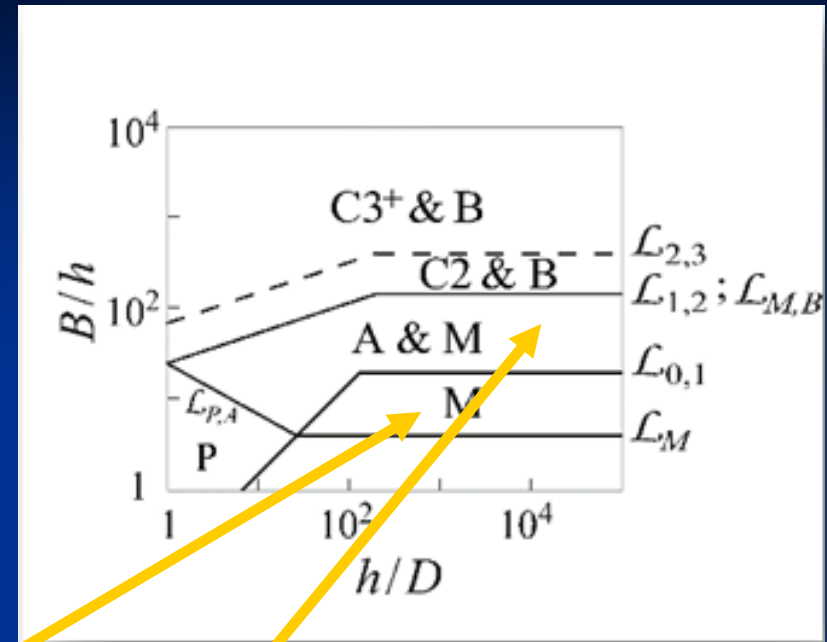
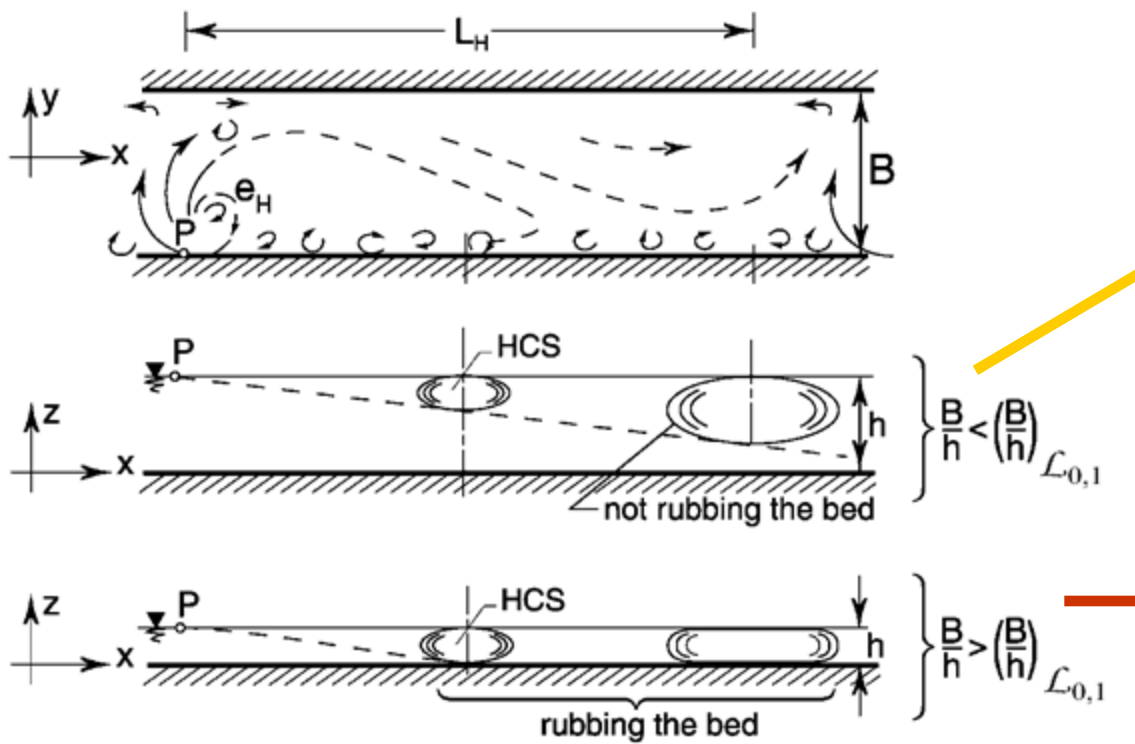
$z/h \approx 0.5$



$z/h \approx 0.2$



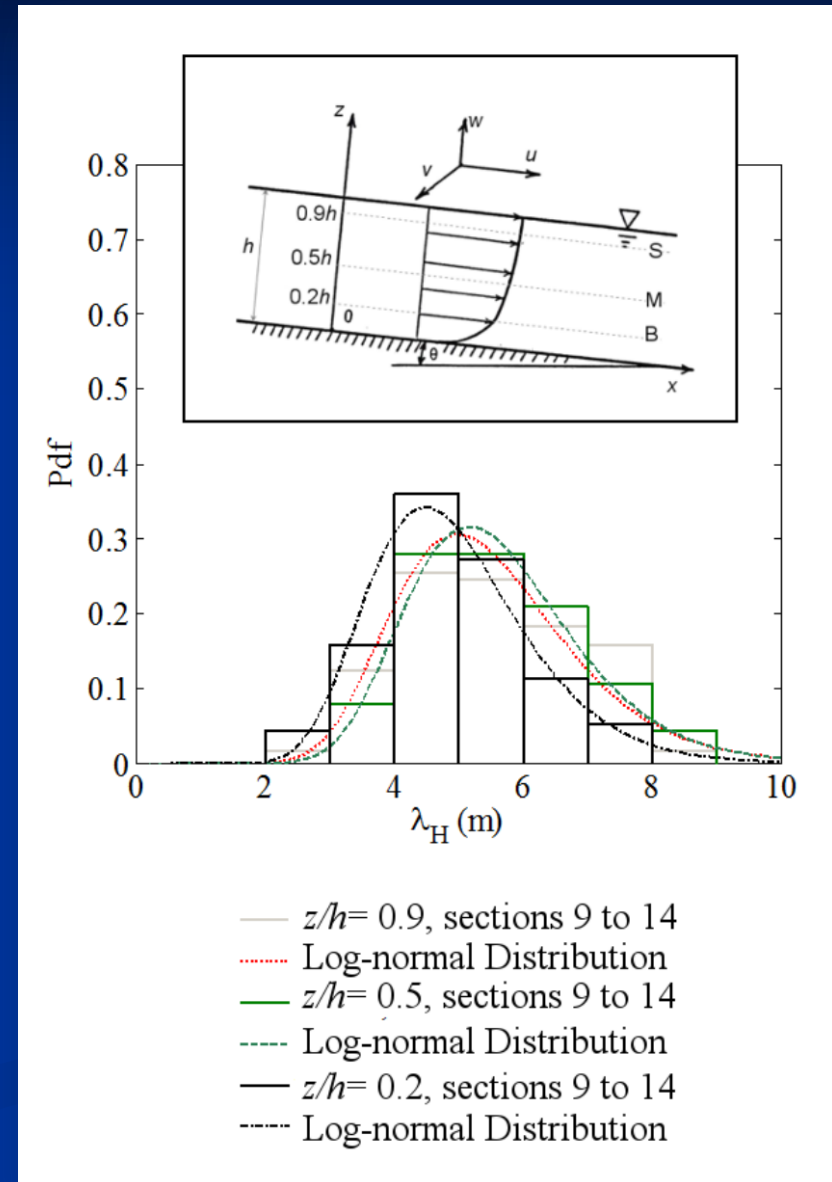
# Conclusion



# Deep flow results: Variation of flow structure over the flow depth

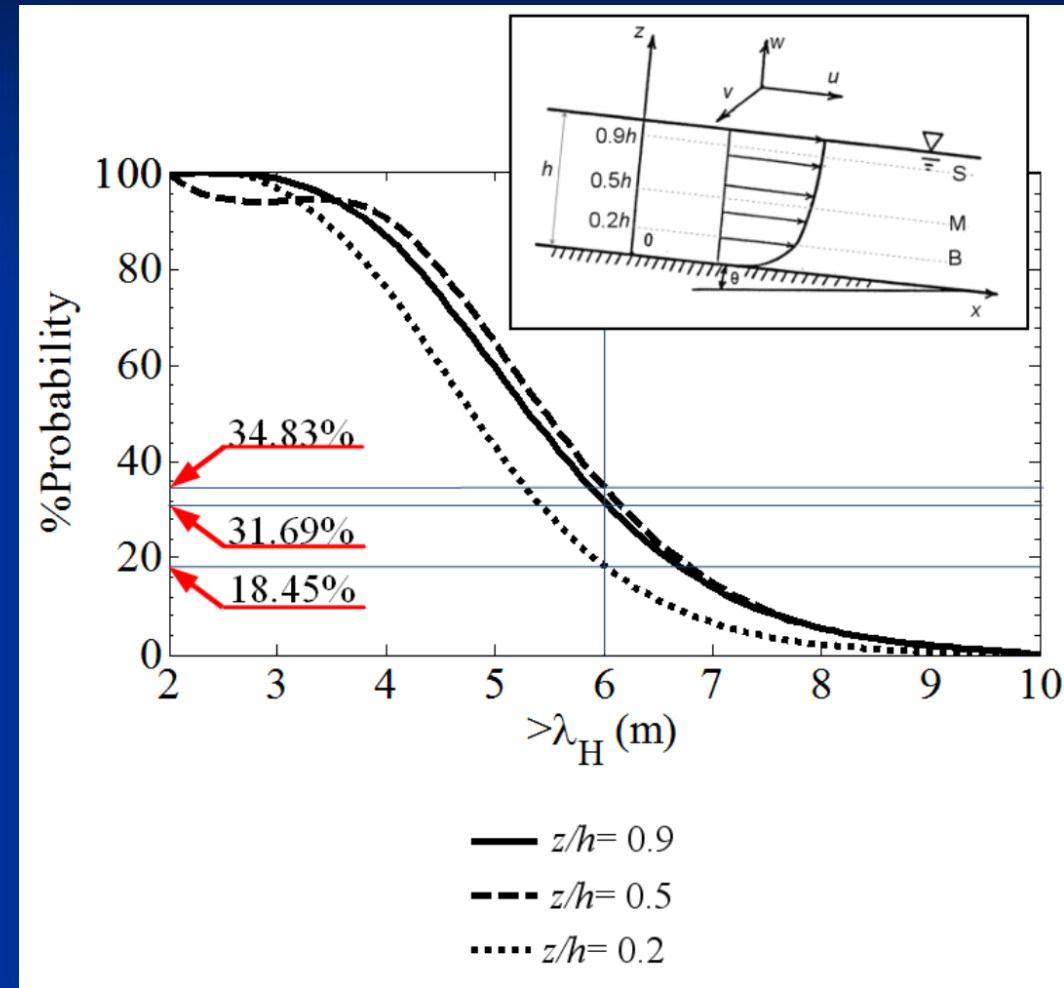
For the sections 9 to 14 and stations 1 to 19, the average burst length of HCS's ( $\lambda_H$ ) was found using the fitted distributions on the probability density functions (Pdf's) of  $\lambda_H$ .

$z/h$	$\lambda_H/B$
0.9	5.5
0.5	5.6
0.2	4.9



# Deep flow results: Variation of flow structure over the flow depth

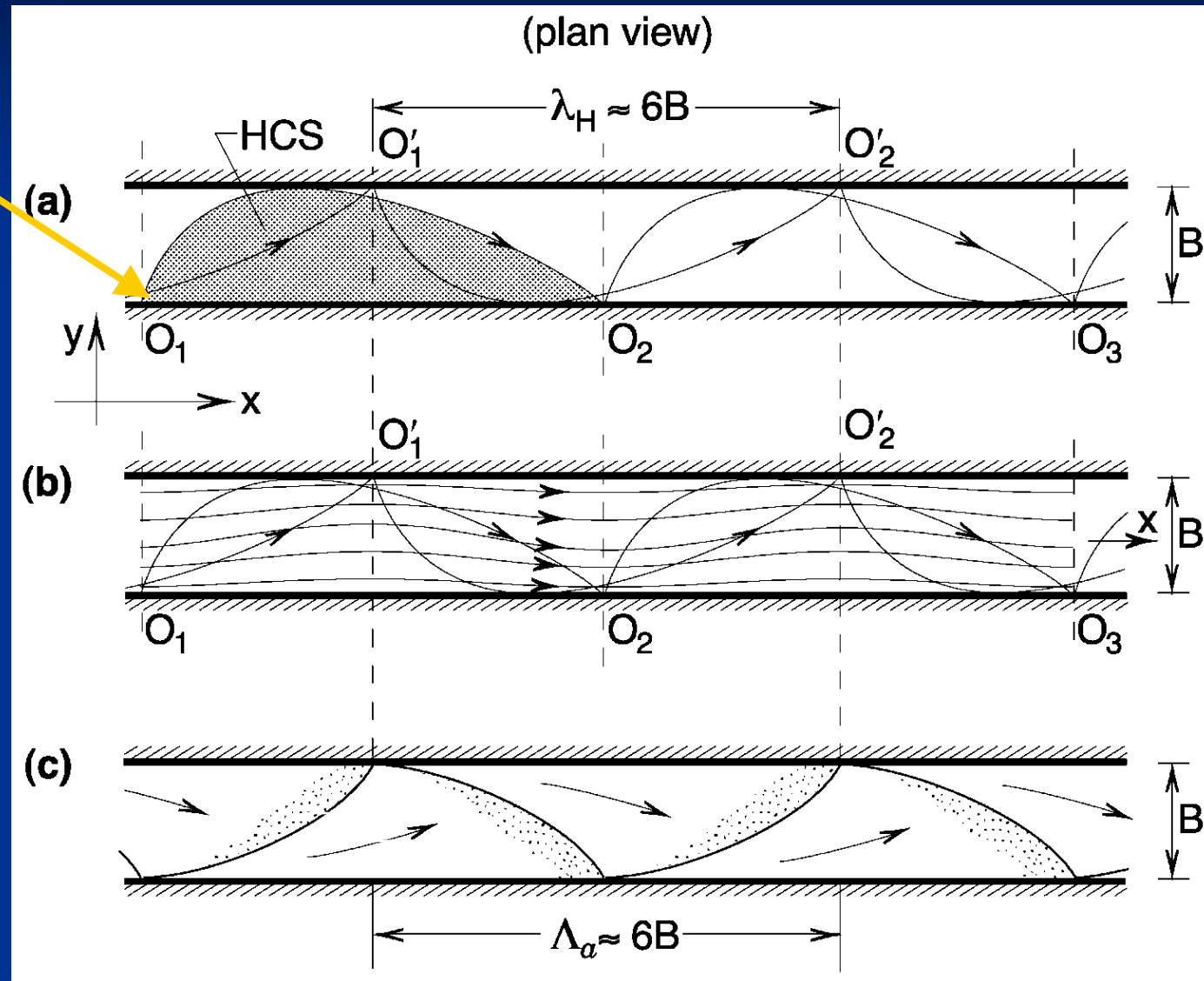
- The probability of the existence of HCS's with length-scales larger than specific value was calculated by integration the area under the Pdf's curves.
- As an example, at the level  $z/h \approx 0.9$ , the probability of existence of a HCS with an average length-scale equal or larger than 6 m  $\approx 31.7\%$
- The probability of the existence of HCS's with an average length-scale greater than 6 m at the level  $z/h \approx 0.9$  is  $\approx 71\%$  higher than the same length-scale at level  $z/h \approx 0.2$  ( $31.66/18.45=1.71$ ).





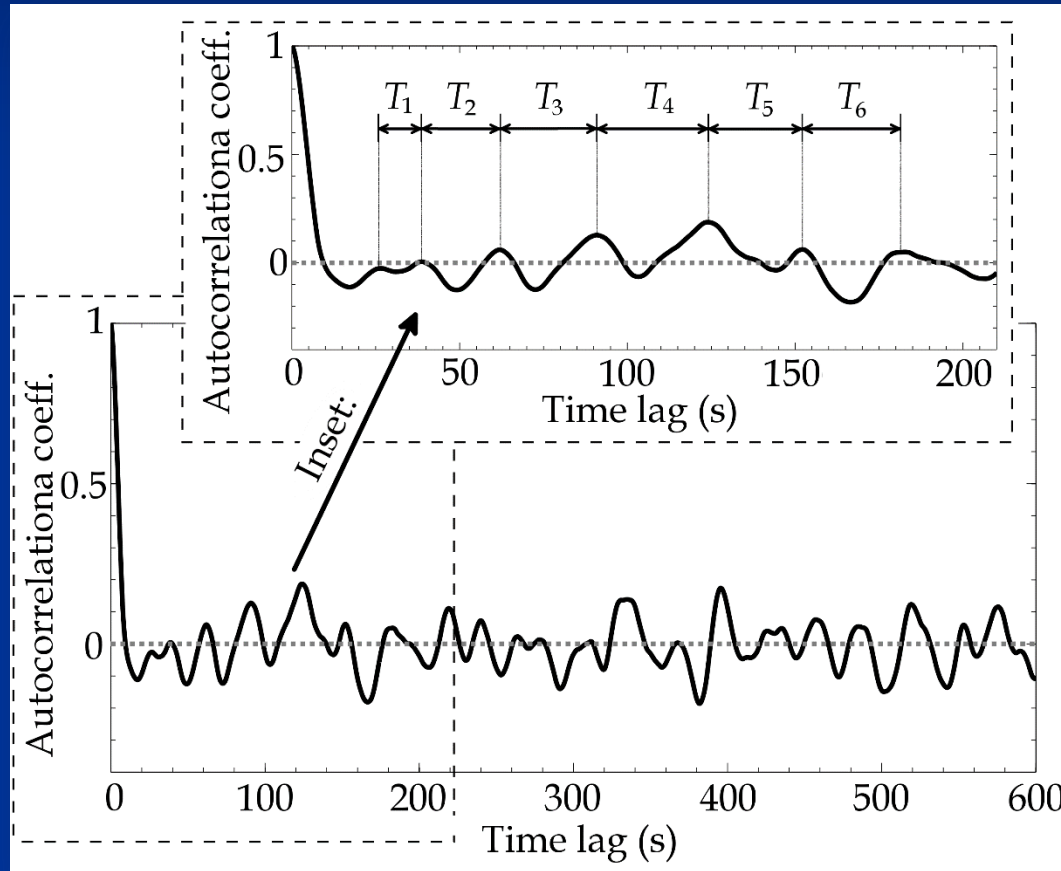
# Location of preference (discontinuity)

- Bursts are randomly distributed in space and time. This means that under completely uniform conditions of flow, there is an equal probability of occurrence of bursts for any region  $\Delta x$  and time interval  $\Delta t$   $\longrightarrow$  homogeneous distribution of bursts  $\longrightarrow$  no wave-like deformation of the flow, and consequently of the bed



# Deep flow results: burst period and burst length

## iii) Temporal autocorrelation function of the smoothed oscillograms



$$R_u(\tau) = \frac{\overline{u'(t) u'(t + \tau)}}{\overline{u'^2(t)}}$$

$$\begin{aligned} T_H &\approx 25.2 \text{ s} \\ &= (T_1 + T_2 + \dots + T_6) / 5 = \\ &= (\approx 13 + \approx 24 + \approx 24 + \approx 33 + \approx 28 + \\ &\approx 29) / 5 \end{aligned}$$

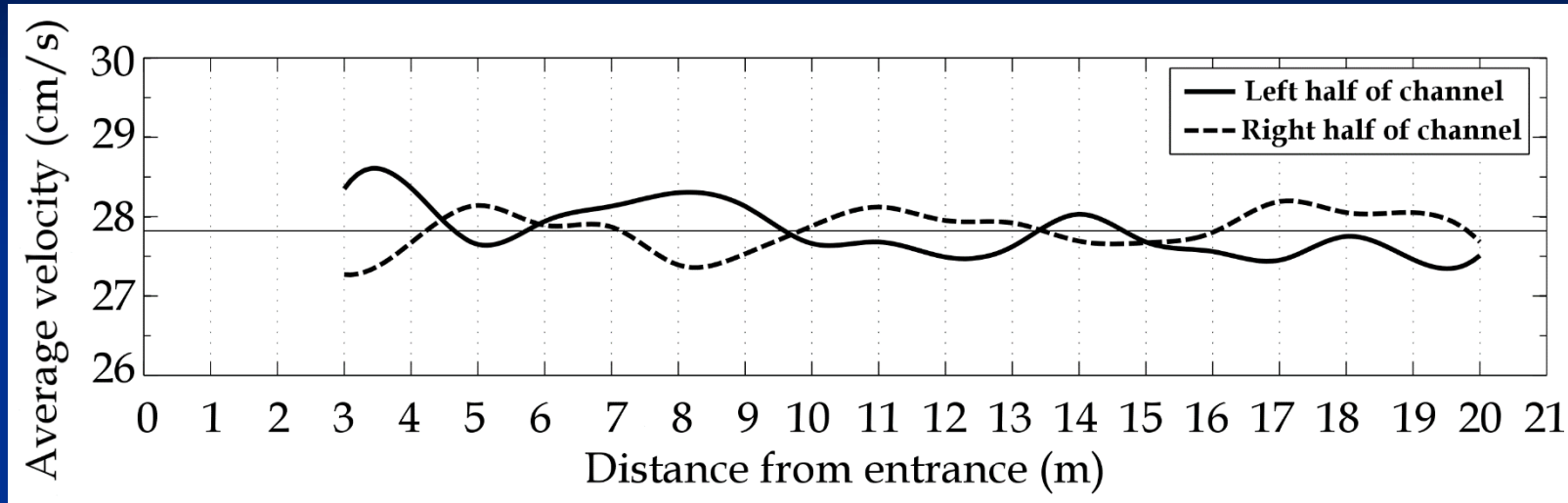
Previous slide:

$$T_H \approx 22.4 \text{ s}$$

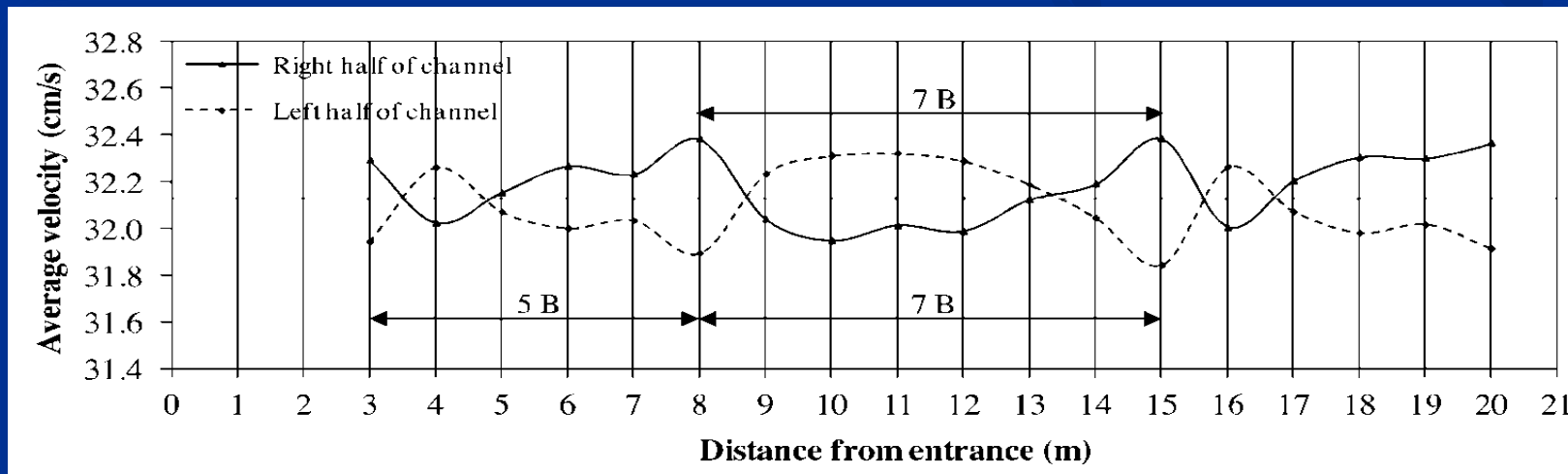
Autocorrelation function at  $z/h \approx 0.9$  for the 20 min long record at section 12, station 10

# Deep flow results: effect of HCS's on the mean flow

- Time-averaged Flow Velocity deep flow:

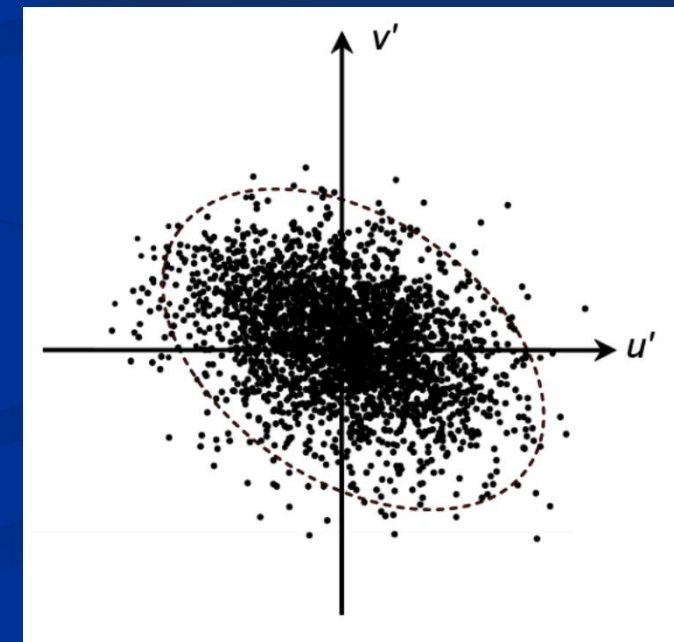
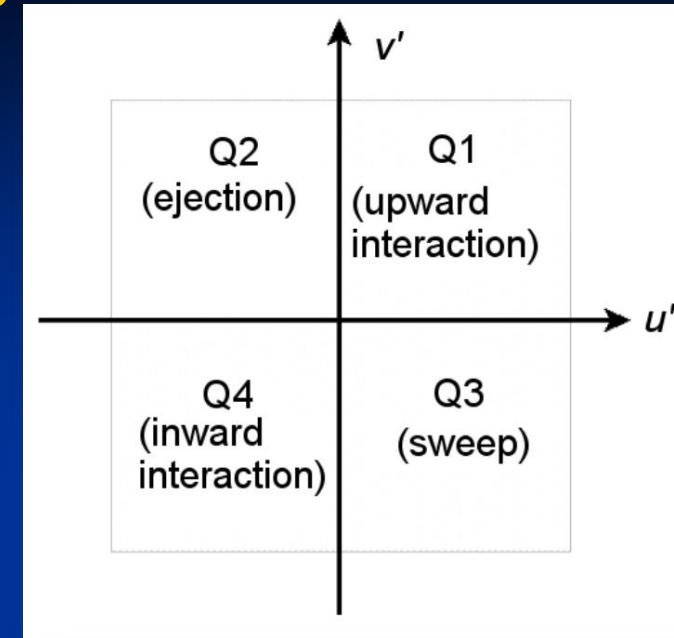


- Time-averaged Flow Velocity shallow flow:



# Deep flow results: Quadrant Analysis

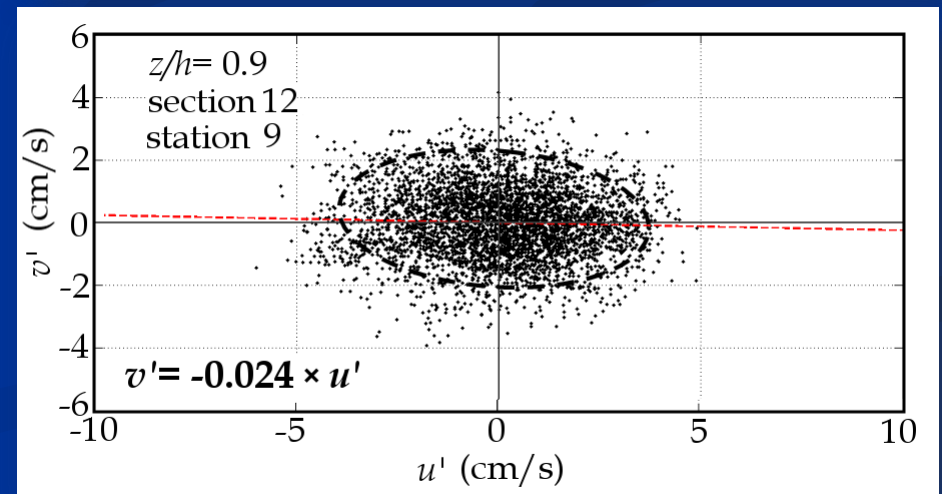
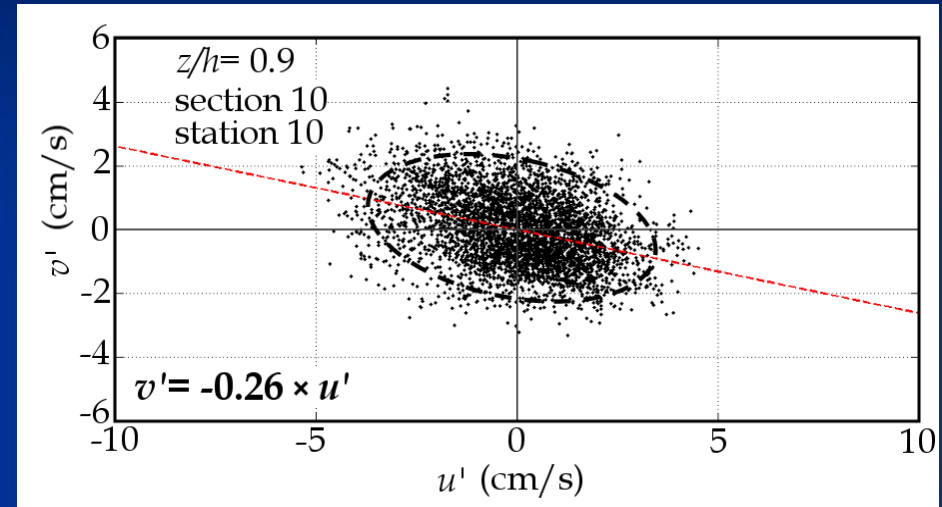
- In open-channel flows, quadrant analysis is used to study the joint behaviour of the longitudinal and vertical fluctuating velocities to investigate the bursting phenomena of VCS's (Nakagawa and Nezu 1993, Buffin-Belanger et al. 2000, Maltese et al. 2007).
- Ahmari (2010), whose study is believed to be the first application of quadrant analysis to the detection of HCS's in open-channel flows, used this technique to investigate the existence of HCS's.
- Ejection ( $u' < 0, v' > 0$ ); Sweep ( $u' > 0, v' < 0$ ); Upward interaction ( $u' > 0, v' > 0$ ); Inward interaction ( $u' < 0, v' < 0$ )



# Deep flow results: Variation of flow structure over the flow depth

## Coherent structures existence index (CSEI)

- If the major axis (or transverse diameter) of the hypothetical ellipse representing the data on the quadrant planes exhibits a slope, then that implies the more frequent occurrence of specific events related to coherent structures out of the four following possibilities.
- when the slope approaches to zero the data are almost evenly distributed in all quadrants, then that either reflects a large influence of flow structures associated with opposite shear layers, or incoherent background flow structures.



# Deep flow results: Variation of flow structure over the flow depth

Coherent structures existence index (CSEI):

The absolute value of the aforementioned slope can be used as an index to quantify the existence of coherent structures or their tendency to possible events.

$z/h$	CSEI
0.9	0.178
0.5	0.051
0.2	0.034

For sections 9 to 14 and stations 1 to 19, the average value of CSEI at  $z/h \approx 0.9$  is **3.5** and **5.2** times higher than that at levels  $z/h \approx 0.5$  and  $z/h \approx 0.2$ , respectively.

